ADVANCED ENERGY MATERIALS
www.advenergymat.de

Reducing External Pressure Demands in Solid-State Lithium Metal Batteries: Multi-Scale Strategies and Future Pathways

Pan Xu, Chen-Zi Zhao, Xue-Yan Huang, Wei-Jin Kong, Zong-Yao Shuang, Yu-Xin Huang, Liang Shen, Jun-Dong Zhang, Jiang-Kui Hu, and Qiang Zhang**

Solid-state lithium metal batteries (SSLMBs) are poised to revolutionize energy storage technologies by combining exceptional energy density with inherent safety. Yet, their commercialization faces fundamental challenges: poor solid–solid interfacial contacts, lithium dendrite proliferation, and electro-chemo-mechanical failure. This perspective presents a comprehensive analysis of external pressure as a multi-scale engineering lever for SSLMBs, bridging atomic-level ion transport, interfacial stabilization, and industrial-scale device integration with particular emphasis on its dynamic interplay with internal stress. At the atomic scale, applied pressure densifies electrode/electrolyte architectures, optimizes ion-transport pathways, and mitigates lattice distortion-induced stresses. Microscopically, it enables intimate interfacial contacts, homogenizes Li deposition stresses to suppress dendrites, and stabilizes interphases. Macro-scale strategies demonstrate how dynamic pressure coupling through in(ex) situ monitoring and roll-to-roll compaction can sustain interfacial integrity in large-area cells by counterbalancing internal stress evolution. External pressure is positioned as a tunable design parameter that synergizes materials innovation with process engineering to simultaneously enhance electrochemical performance and mechanical resilience. Looking ahead, intelligent pressure-management systems integrating machine learning-driven adaptive control, stress-responsive materials, and operando characterization tools is proposed. These advancements will be pivotal for realizing pressure-optimized SSLMBs that meet the energy density (>500 Wh kg^{-1}) and cycling stability demands of electric aviation and grid storage, which will accelerate the global transition to sustainable energy.

1. Introduction

The worldwide push toward sustainable energy systems has spurred intensive research into advanced energy storage technologies capable of meeting the escalating demands for high energy density, safety, and durability.[1] Solid-state lithium metal batteries (SSLMBs) mark a revolutionary change in battery technology,[2] offering transformative advantages in comparison to lithium-ion batteries (LIBs) that can redefine performance benchmarks across industries.[3] The routine LIBs utilizing organic carbonate-based electrolytes exhibit inherent susceptibility to thermal runaway,[4] which culminates in destructive outcomes including combustion or detonation.[5] Notably, a critical innovation addressing longstanding safety concerns at the heart of SSLMBs lies the substitution of combustible liquid electrolytes[6–8] with non-flammable solid-state electrolytes (SSEs).[9, 10] For instance, sulfide-based SSEs such as Li_6PS_5Cl[11] remain stable at temperatures exceeding 200°C, while oxide-based SSEs such as $Li_7La_3Zr_2O_{12}$ (LLZO)[12] demonstrate negligible degradation even under extreme operational stress.[13]

P. Xu, C.-Z. Zhao, X.-Y. Huang, W.-J. Kong, Z.-Y. Shuang, Y.-X. Huang, L. Shen, J.-D. Zhang, Q. Zhang
Beijing Key Laboratory of Complex Solid-State Batteries
Department of Chemical Engineering
Tsinghua University
Beijing 100084, P.R. China
E-mail: zcz@tsinghua.edu.cn; zhang-qiang@mails.tsinghua.edu.cn

C.-Z. Zhao, Q. Zhang
State Key Laboratory of Chemical Engineering and Low-Carbon Technology
Tsinghua University
Beijing 100084, P. R. China

J.-K. Hu
The Innovation Center for Smart Solid State Batteries
Yibin 644002, P. R. China

Q. Zhang
Institute for Carbon Neutrality
Tsinghua University
Beijing 100084, P.R. China

P. Xu
Engineering Research Center of Energy Storage Materials and Devices
Ministry of Education
Engineering Research Center of Energy Storage Materials and Chemistry
School of Chemistry
Xi'an Jiaotong University
Xi'an 710049, P. R. China

The ORCID identification number(s) for the author(s) of this article can be found under https://doi.org/10.1002/aenm.202504613

DOI: 10.1002/aenm.202504613

The intrinsic safety of solid electrolytes renders SSLMBs indispensable for practical applications where reliability is paramount,[14, 15] including electric vehicles (EVs), aerospace systems, and grid-scale energy storage.[16] Beyond safety, SSLMBs unlock unprecedented energy density by leveraging metallic lithium (Li: theoretical specific capacity of 3860 mAh g^{-1}) as the anode,[17] when integrated with high-voltage cathodes such as $LiNi_{0.8}Mn_{0.1}Co_{0.1}O_2$ (NMC811), SSLMBs achieve energy densities exceeding 500 Wh kg^{-1},[18] a critical threshold that remains infeasible for routine liquid electrolyte systems owing to irreversible parasitic reactions and dendrite formation.[19] Besides, SSEs mitigate the side reactions of electrode–electrolyte by forming stable interfaces in SSLMBs.[20] For instance, polymer-based SSEs[21] like polyethylene oxide (PEO) paired with Li salts exhibit minimal interfacial degradation, enabling over 1000 cycles with >80% capacity retention,[22] this durability is particularly advantageous for practical applications requiring long-term reliability. In addition, the environmental impact of SSLMBs also aligns with global sustainability goals. Liquid LIBs rely on toxic solvents and pose recycling challenges due to their complex chemistry.[23] SSLMBs, however, utilize inorganic[24] or polymer[25] SSEs that are easier to reclaim. The SSLMBs represent a convergence of safety, energy density, and sustainability, positioning them as the cornerstone of next-generation energy storage.[26] Despite these advantages, however, SSLMBs face hurdles that delay widespread adoption.

Specifically, key challenges include inferior interfacial contacts between electrode particles and electrode/electrolyte interface,[27] Li dendrite penetration through SSEs, and chemo-mechanical degradation during cycling.[28] To tackle these problems, external pressure has risen as a transformative regulation parameter, which acts across multiple-scales to optimize performance. Among them, the external pressure[29] in SSLMBs is categorized into two regimes: (I) preparation pressure (10–500 MPa), applied to densify microstructures during the fabrication of electrode materials and SSEs,[30] and (II)[31] stack pressure (0.1–10 MPa), maintained to stabilize dynamic interfaces during operation.[32] Notably, the external pressure is often a passive compensation strategy to mitigate inherent material limitations, rather than an ideal active design principle. Additionally, it is critical to distinguish external pressure from internal stress when analyzing their roles in SSLMBs,[33] as their distinct origins and action scales directly influence battery performance. External pressure refers to macro-scale mechanical forces applied to the entire battery system (e.g., stack pressure from fixtures or isostatic holders), primarily regulating overall compaction, eliminating macroscopic voids, and ensuring large-area electrode-electrolyte contact. In contrast, internal stress arises from localized chemo-mechanical interactions within the battery, driven by electrochemical reactions (e.g., volume expansion of anode or cathode particles during lithiation, Li plating/stripping in metal anode) or structural inhomogeneities (e.g., grain boundary mismatch in SSEs). This internal stress acts at multi-scales, concentrating at interfaces, particle contacts, or defect sites, and can induce microcracking, interfacial delamination, or dendrite nucleation if unmanaged. The interplay between external pressure and internal stress is pivotal: external pressure can alleviate harmful internal stress (e.g., suppressing cracks via compaction) but may exacerbate it if mismatched (e.g., excessive pressure amplifying stress at cathode particle edges), while tailored internal stress (e.g., via gradient material design) can reduce reliance on external pressure.

In light of this, the integration of external pressure into SSLMBs transcends mere mechanical intervention, which constitutes a multiscale coordination framework for harmonizing atomic-, micro-, and macro-scale interactions across electrode components and internal battery architectures. To comprehensively illustrate the evolution and milestones of external pressure application in SSLMBs, **Figure 1** presents a detailed roadmap, highlighting key breakthroughs and advancements that have propelled the field from fundamental understanding to practical implementation.[30] Specifically, in 2013, Tatsumisago et al. explores sulfide SSE pressure responsiveness—cold pressing enables room-temperature densification, boosts ionic conductivity by reducing grain boundary resistance, and provides mechanical parameters;[34] In 2019, Harris et al. proposes contact mechanics model breaks "conformal contact" assumption, clarifying local asperity stress (far higher than macro-pressure) suppresses dendrites;[35] In 2021, Zhang et al. presents mechano-electrochemical phase field model elucidates pressure's dual effects and establishes "electrolyte modulus-critical pressure" phase diagram;[36] In 2023, Hatzell et al. validates high-pressure efficacy—pressure and elevated temperature fills stripping voids to inhibit interface failure;[37] In 2024, Meng et al. develops a device that can uniformly and controllably regulate the pressure during the cycle process;[38] Furthermore, in 2025, Wang et al. adopts in situ TEM testing to analyze the lithium deposition behavior mechanism under different external pressures,[39] and the aforementioned representative advancements have laid the foundation for the future realization of low/non-external pressure-dominated for >500 Wh kg^{-1}, >1000 cycles and high-safety solid-state lithium metal batteries.

Synchronously, it elucidated how research efforts have progressively refined pressure strategies to optimize battery performance. The external pressure reconfigures ion transport pathways by compressing lattice structures and reducing activation energy barriers at the atomic scale. For instance, the preparation pressure densifies SSEs by collapsing voids between particles, a process critical for sulfide-based SSEs like Li_6PS_5Cl, where ionic conductivity scales nonlinearly with applied force due to enhanced particle-particle contacts.[41] The stack pressure, meanwhile, dynamically adjusts interfacial atomistic arrangements. When lithium ions traverse the Li||SSEs interface under applied pressure, compressive stress rectifies surface irregularities and suppresses electron leakage, consequently lowering energy dissipation.[42] This mechanism, analogous to "mechanical doping", effectively optimizes charge transfer kinetics through coordinated physicochemical regulation.[43] On the micro-scale, the external pressure governs interfacial morphology and stability. Among them, the preparation pressure ensures uniform electrode-electrolyte adhesion by embedding active particles into the SSEs matrix, a process vital for high-voltage cathodes such as $LiNi_{0.8}Mn_{0.1}Co_{0.1}O_2$ (NMC811). However, insufficient preparation pressure induces protrusion of micron-sized cathode particles, creating localized stress concentrations that fracture SSEs during cycling.[44] Therefore, the stack pressure counteracts these effects by inducing creep deformation in metallic Li, which adaptively fills interfacial gaps formed during volume changes. Notably, this self-healing mechanism is particularly crucial for

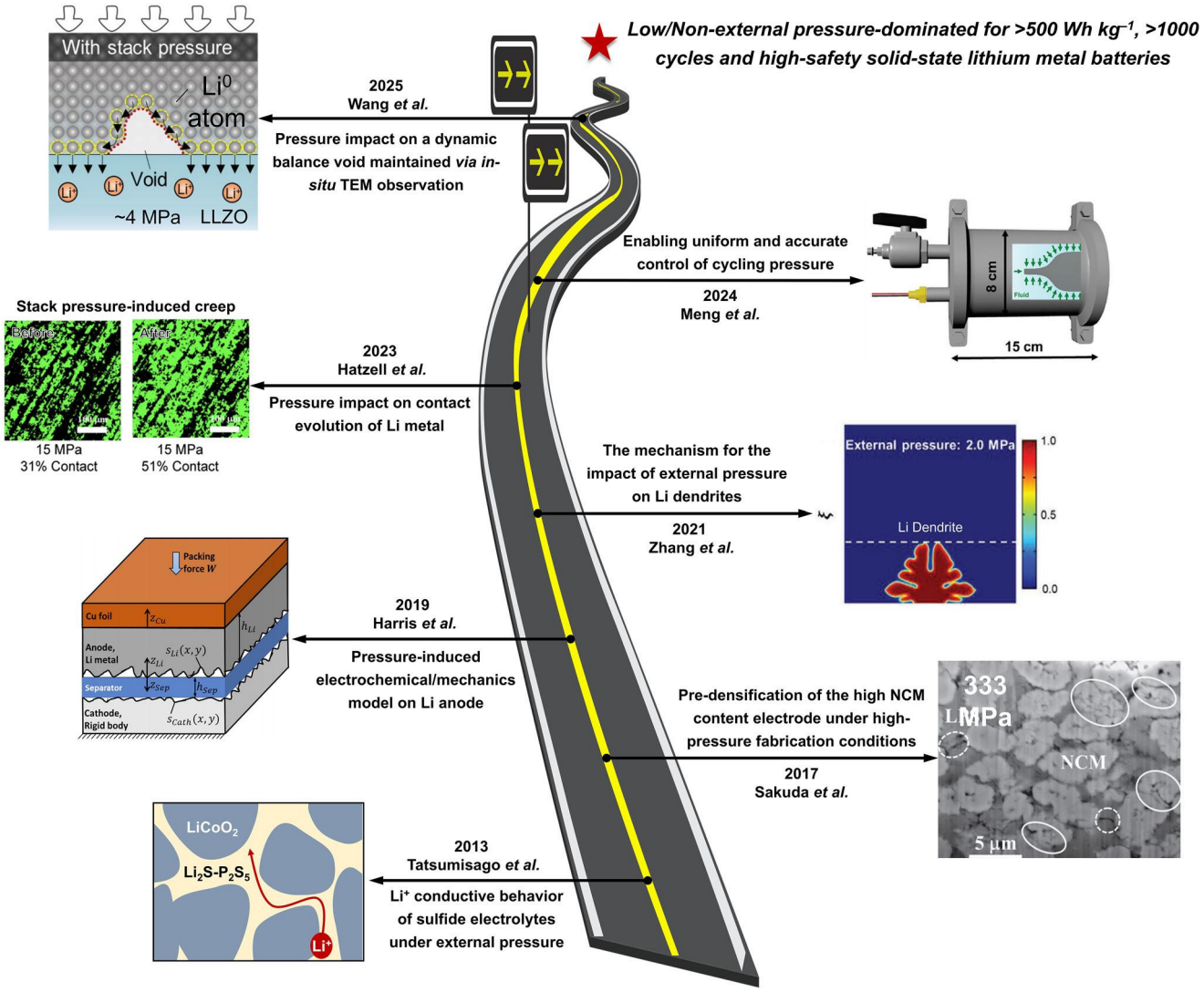

Figure 1. The critical development history of external pressure on SSLMBs from 2013s to the future. Reproduced with permission.[34] Reproduced with permission.[40] Copyright 2017, The Ceramic Society of Japan; Reproduced with permission.[35] Copyright 2019, The Electrochemical Society; Reproduced with permission.[36] Copyright 2021, Wiley-VCH; Reproduced with permission.[37] Copyright 2023, American Chemical Society; Reproduced with permission.[38] Copyright 2024, Wiley-VCH; Reproduced with permission.[39] Copyright 2025, American Association for the Advancement of Science.

alloy anodes (e.g., Si, Sn, etc.), where pressure inhibits Li dendrite growth by redistributing stress gradients.[45] At the macro-scale, the external pressure governs the transition from material characteristics to production viability. The preparation pressure determines the scalability of SSEs, among them, the thick, porous architectures require higher pressures to achieve target ionic conductivities, escalating manufacturing costs.[46] Conversely, the stack pressure introduces practical challenges: maintaining uniform pressure across industrial-scale cells demands innovative cell designs, such as spring-loaded fixtures or pneumatic systems, which add complexity to battery packs.[47] Collectively, while external pressure optimizes the performance of SSLMBs, its effects are material- and scale-dependent.[48] Sulfide-based SSEs, with their ductile nature, achieve near-theoretical ionic conductivity under high preparation pressures (100–400 MPa). However, excessive pressure (>500 MPa) fractures brittle oxide-based SSEs such as $Li_7La_3Zr_2O_{12}$ (LLZO), creating short-circuit pathways.[49] Similarly, the stack pressures (>10 MPa) suppress Li dendrites growth in sulfide-based SSLMBs but accelerate Li creep into the defect of SSE.[50] Moreover, polymer SSEs present unique challenges, which viscoelasticity allows moderate stack pressures (1–5 MPa) to enhance interfacial contacts, but prolonged pressure induces irreversible chain entanglement, reducing ionic mobility.[51] Hence, optimizing interfacial stability while maintaining ionic transport necessitates hybrid pressure strategies, such as combining high initial preparation pressure with adaptive stack pressure modulation. Advancing such strategies, the future of SSLMBs lies in smart pressure control systems capable of dynamically adjusting force profiles based on operational states. For instance, machine learning algorithms can optimize stack pressure in real-time by correlating impedance data with mechanical response, thereby mitigating dendrite growth

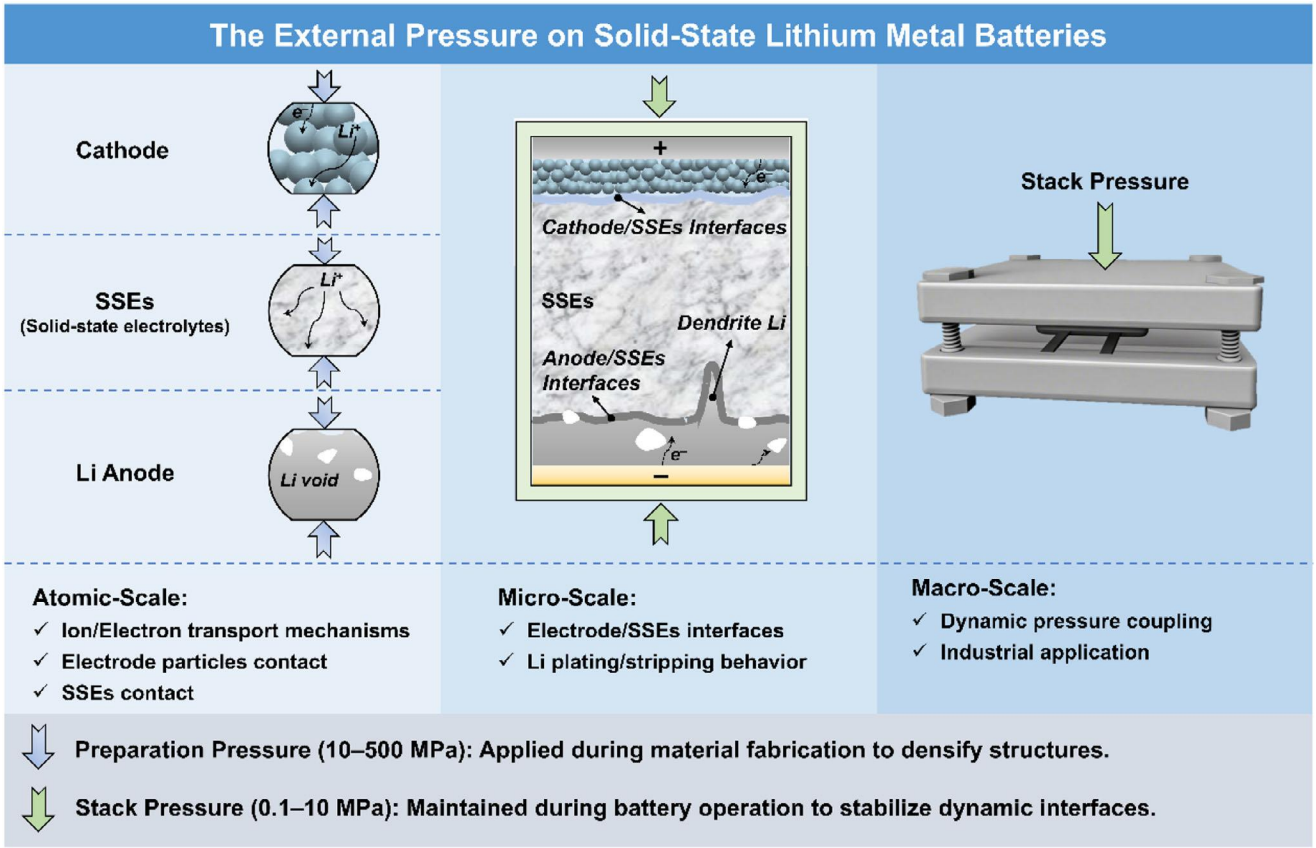

Figure 2. The schematic representation of the multi-scale effects of external pressure on SSLMBs.

during fast charging.[52] Furthermore, material-by-design approaches, such as solid-state electrolytes with graded mechanical properties, can decouple preparation and operational pressure requirements, ultimately enabling a controlled pressure-dominated SSLMB architectures.

In this perspective, the multi-scale role of external pressure in SSLMBs is systematically elucidated from atomistic ion transport mechanisms to working devices (**Figure 2**). The external pressure modifies ion/electron transport mechanisms at particulate interfaces at atomic-scale, altering electrode structures. On the micro-scale, the external pressure impacts interfacial contacts and Li plating/stripping behavior, influencing the formation of the solid-state electrolyte interphase (SEI) and dendrite suppression. At the macro-scale, the external pressure is vital for building a robust pouch cell and pack. By understanding these effects, this perspective aims to afford valuable insights into the role of external pressure in SSLMBs, guiding both academic research and industrial development toward the realization of high-performance, pressure-optimized, and even pressure-free SSLMBs.

2. Atomic-Scale Insights: The Pressure-Induced Ion/Electron Transport Mechanisms at Particulate Interfaces

The efficient transport of ions and electrons at the particulate interfaces of SSLMBs is fundamentally governed by atomic-scale interactions, where external pressure emerges as a pivotal regulator of structural and chemical dynamics.[53] At this scale, pressure-induced modifications in lattice geometry, defect concentration, and interfacial bonding profoundly determine the electrochemical performance of cathode particles,[54] anode particles, and solid-state electrolytes (SSEs).[55] By dissecting these mechanisms, we uncover how external pressure reshapes the energy landscapes for ion migration, electron transfer, and phase stability, thereby dictating the overall kinetics and durability of SSLMBs. Notably, these effects are primarily mediated through improved interfacial contacts rather than direct alteration of intrinsic material properties.

2.1. Cathode Particles

The external pressure profoundly influences the ion and electron transport mechanisms within cathode particles, primarily by modulating interfacial contacts, particle morphology, and lattice dynamics. These effects are critical for optimizing the electrochemical performance of SSLMBs, where solid-solid interfaces inherently suffer from high resistance and poor wetting compared to liquid electrolyte systems.

In composite cathodes, the external pressure is applied during fabrication and operation, i.e. preparation/stack pressure (**Figure 3a**). This directly impacts the packing density and cathode particle-particle contacts. Mukherjee et al. demonstrated that

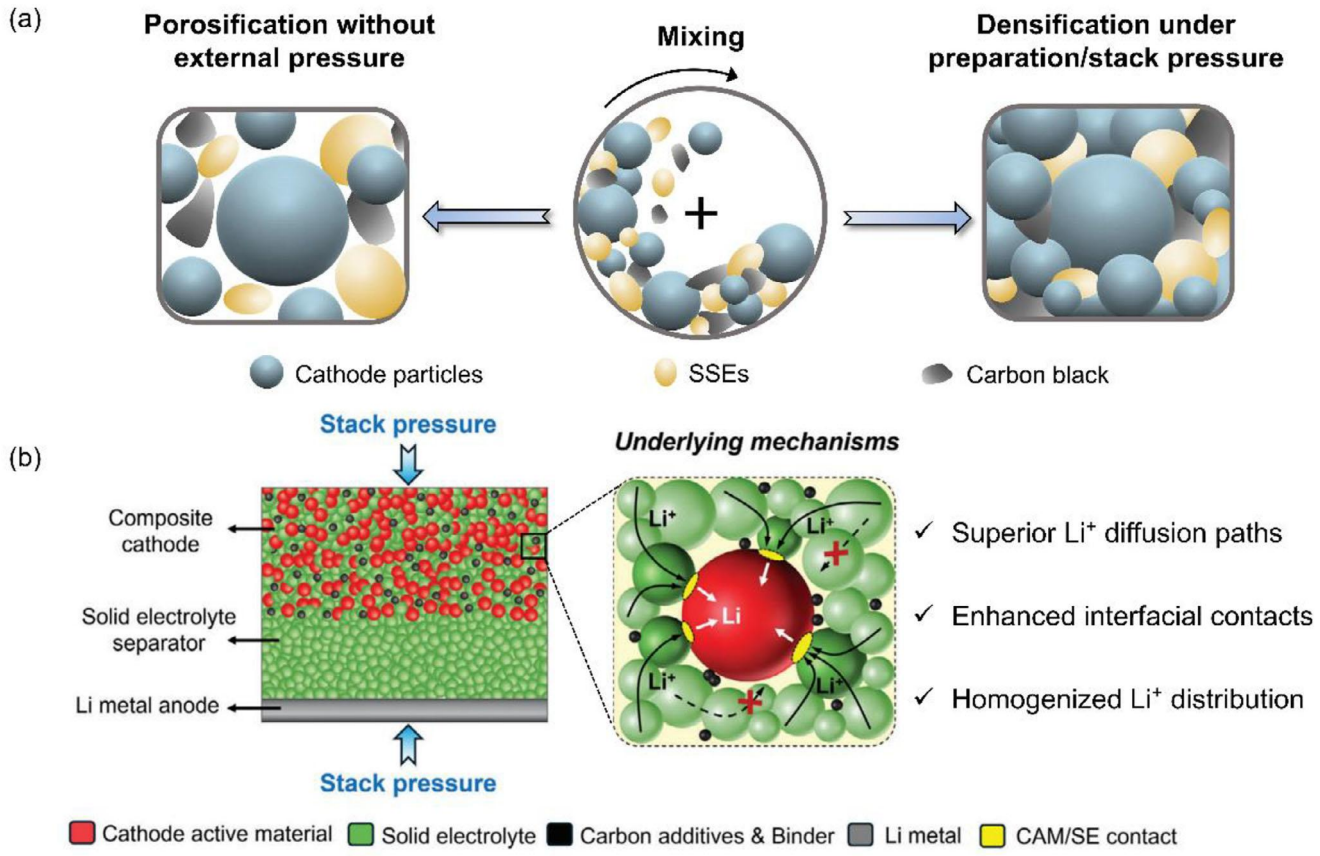

Figure 3. The atomic-scale of cathode particles. a) The schematic of mixing the composite cathode with/without the external pressure. b) The stack pressure (12 MPa) enhances ion transport across solid-solid interfaces in SSLMBs. Reproduced with permission.[44] Copyright 2021, Wiley-VCH.

low pressure (1.0 MPa) leads to limited cathode-active-material (CAM)/SSE contacts, causing prolonged Li^+ diffusion paths and localized reactions within single-crystal NMC532 particles, which increases interfacial resistance and polarization. However, enhanced contact homogenizes Li^+ distribution (Figure 3b) and improves capacity utilization under higher pressures (12 MPa).[56] For this, systematic exploration of how fabrication pressure affects composite cathodes by using $LiNi_{1/3}Co_{1/3}Mn_{1/3}O_2$ (NCM) and sulfide-based solid-state electrolytes, finding that moderate fabrication pressure (37 MPa) improved particle densification and reduced interfacial voids, thereby enhancing ionic conductivity through increased solid-solid interface contact. However, excessive fabrication pressure (>100 MPa) caused NCM particle fracturing, creating isolated regions that disrupt ion transport and raise interfacial resistance.[40] Such findings highlighted the critical need to balance densification and particle integrity, with optimal external pressure ensuring both percolating ion pathways and structural stability. Notably, cathode particles generate internal stress during cycling due to lattice expansion/contraction, which concentrates at grain boundaries and interfaces. This internal stress can exacerbate crack formation in poly-crystal (PC) NCM under pressure, whereas the structural homogeneity of single-crystal (SC) NCM reduces internal stress accumulation, explaining their superior mechanical resilience and stable ion transport. For instance, SC-NCM particles coated with $LiNbO_3$ maintained intimate contacts with Li_6PS_5Cl electrolytes even at low stack pressures (2.5 MPa), achieving a high discharge capacity of 210 mAh g^{-1} and >99% Coulombic efficiency after the initial cycle. The uniform deformation of SC particles under pressure suppressed intergranular cracking, unlike PC-NCM, which suffered from particle fragmentation and contact loss at grain boundaries. This structural homogeneity reduced charge transfer resistance, as evidenced by impedance spectra showing smaller interfacial resistance (R_{PE}≈40 Ω cm^2) compared to PC-NCM (R_{PE}≈80 Ω cm^2).[57] Further comparison the electro-chemo-mechanical behavior of SC and PC NCM811 in $Li_{10}SnP_2S_{12}$-based SSLMBs, revealing that SC-NCM retained higher capacity retention (64.5% after 100 cycles at 4.35 V) due to the reduced anisotropic volume change and pressure-induced grain boundary stabilization.[44] The external pressure facilitated the construction of a more uniform SEI, minimizing interfacial degradation and maintaining continuous ion transport pathways. In contrast, PC-NCM undergoes rapid capacity fade due to pressure-induced microcracks and SEI instability, underscoring the synergy between particle microstructure and pressure effects. Beyond contact and structural effects, the external pressure also modifies lattice parameters and defect formation in cathode particles, influencing ion migration barriers. For $LiNi_{0.83}Mn_{0.06}Co_{0.11}O_2$ cathodes in Li_3InCl_6 electrolytes, increased pressure reduces lattice spacing and enhanced Li^+ diffusion by suppressing oxygen vacancy formation.[58] The pressure-dependent conductivity revealed that higher pressure

(10 vs 2 MPa) reduced the charge transfer resistance, attributed to improved crystallographic alignment and reduced tortuosity of ion pathways. Notably, the increase in charge transfer resistance caused by low stack pressure (2 MPa) can be alleviated by elevating the operating temperature, which increasing the temperature from 30 to 80 °C enhances the ionic conductivity of the sulfide electrolyte (e.g., Li_6PS_5Cl) by reducing the Li^+ migration barrier, thereby compensating for the insufficient interfacial contact induced by low pressure and restoring the charge transfer kinetics.[58]

2.2. Anode Particles

External pressure has a significant impact on the electrochemical and mechanical behavior of anode particles in SSLMBs, particularly governing the stability of Li plating/stripping, interfacial contacts, and structural integrity during cycling, and a key aspect is its interaction with the internal stress inherently generated by anode materials during operation. For lithium metal anodes, plating induces compressive internal stress at the anode/SSE interface that concentrates at defect sites and drives dendrite nucleation if unregulated, while alloy anodes like Si undergo massive volume expansion during lithiation, generating tensile internal stress that leads to particle fracturing and contact loss without mechanical constraint, and external pressure acts as a targeted countermeasure by applying tailored magnitudes to balance these internal stress effects. Unlike cathodes, anode particles including graphite, metallic Li and alloy-based materials such as Si, Sn, In, etc. exhibit unique responses to pressure due to their distinct deformation mechanisms and volume change characteristics.[59] These effects are critical for mitigating dendrite formation, enhancing interfacial ion transport, and ensuring reversible capacity retention.

Based on this, the external pressure addresses these issues by modulating the plastic deformation of Li and grain boundary dynamics. Greer et al. demonstrated that Li pillars exhibit a strong size-dependent yield strength, reaching 105 MPa at room temperature, an order of magnitude greater than bulk Li.[60] This size effect arises from dislocation confinement in small-scale structures, enhancing resistance to dendritic penetration into SSEs. Mechanistically, the external pressure influences the elastic anisotropy of Li and creep behavior: measurements the shear modulus of polycrystalline Li as 2.83 GPa, a key parameter for predicting dendrite suppression via SSE stiffness.[61] Under high external pressure, the grain boundaries of Li act as sinks for dislocations, reducing stress concentrations and delaying void nucleation, as supported by in situ X-ray microscopy showing pressure-induced densification minimizes interfacial cracks even during repeated stripping/plating cycles.[46] Moreover, alloy anodes such as Si, Sn, and Sb undergo significant volume expansions (200–300%) during lithiation, leading to pulverization and contact loss without mechanical constraint. The external pressure exerts a dual effect in such systems: suppressing porosity formation and enhancing ion transport kinetics. In Sb-based composite anodes, the high stack pressure densifies active materials, reducing interfacial resistance and improving capacity retention.[62] Although alloy anodes exhibit severe volume expansion during lithiation, moderate to low stack pressure (0.1–5 MPa) can mitigate this challenge by two key mechanisms: 1) suppressing the formation of internal pores caused by volume expansion via plastic deformation of the anode matrix; 2) maintaining intimate contact between anode particles and SSEs to avoid contact loss. For Si anodes, 0.6 MPa external pressure optimizes particle packing, achieving superior electrical contact during cycling while avoiding electrolyte compaction-induced ion blockage.[45] Additionally, designs incorporating a Mg sacrificial layer beneath Si–graphite composites leverage pressure-induced Li–Mg alloying at the interface to reduce nucleation overpotential, enabling stable cycling at 3 MPa.[63] Similarly, MoS_2 nanosheets forming a Li_2S/Mo interlayer enhance Li wettability and suppress dendrites growth under low external pressure.[64] For sulfide-based SSEs, the external pressure modulates ion conductivity and interfacial reaction kinetics. Sakamoto et al. employed in situ galvanostatic electrochemical impedance spectroscopy (GEIS) and distribution of relaxation times (DRT) analysis to reveal the pressure-dependent evolution of interfacial voids during Li stripping. As shown in **Figure 4a**, at low pressures (<3 MPa), the deep voids emerged rapidly, indicating rapid degradation of interfacial contacts. In contrast, the deep void signals were delayed at high pressures (3–10 MPa) dominated by shallow voids, suggesting external pressure suppresses deep void formation via enhanced Li creep, maintaining interfacial contact stability.[65] To address practical constraints of high-pressure operation, nanostructured anodes and interfacial regulation have been explored. McDowell et al. conducted a systematic study on how stack pressure on Li dealloying behavior in solid-state and liquid electrolyte batteries using Li–Al, Li–Sn, Li–In, and Li–Si alloys. The dealloying induced bicontinuous porosity in metals such as metallic In, enhancing Li diffusion while maintaining mechanical integrity at low pressures (0.5–2 MPa). While higher pressures (10–30 MPa) promoted densification via plastic collapse and solid-state diffusion, suppressing deep voids formation (Figure 4b).[66]

This mechanistic understanding of pressure-driven densification and porosity control inspired subsequent efforts to replicate such effects through structural design rather than external force. Notably, Jung et al. proposed a Si anode design for low-pressure ASSBs, integrating a thin Ag interlayer and Si prelithiation. The Ag interlayer lithiates in situ to form Li_xAg, maintaining Si-SSEs interfacial contact and suppressing SE-CNT side reactions. Prelithiation offsets cycling Li loss, boosting stability. Ag-coated Si anodes outperform bare ones under low pressure, offering a practical framework for high-energy ASSBs.[68] Furthermore, Chen et al. proposed a $Li_{21}Si_5$/Si-$Li_{21}Si_5$ bilayer anode, in which the bottom Si-$Li_{21}Si_5$ layer establishes a 3D continuous conductive network, the top $Li_{21}Si_5$ layer acts as a mixed ionic/electronic conductor to homogenize interfacial electric fields, facilitating a twofold increase in lithium-ion flux. This design enables integrated ion-electron co-transport, eliminating reliance on external pressure while achieving stable cycling (Figure 4c),[67] offering an innovative framework for pressure-free all solid-state batteries and illustrating how architectural design can optimize transport mechanisms and mechanical stability simultaneously.

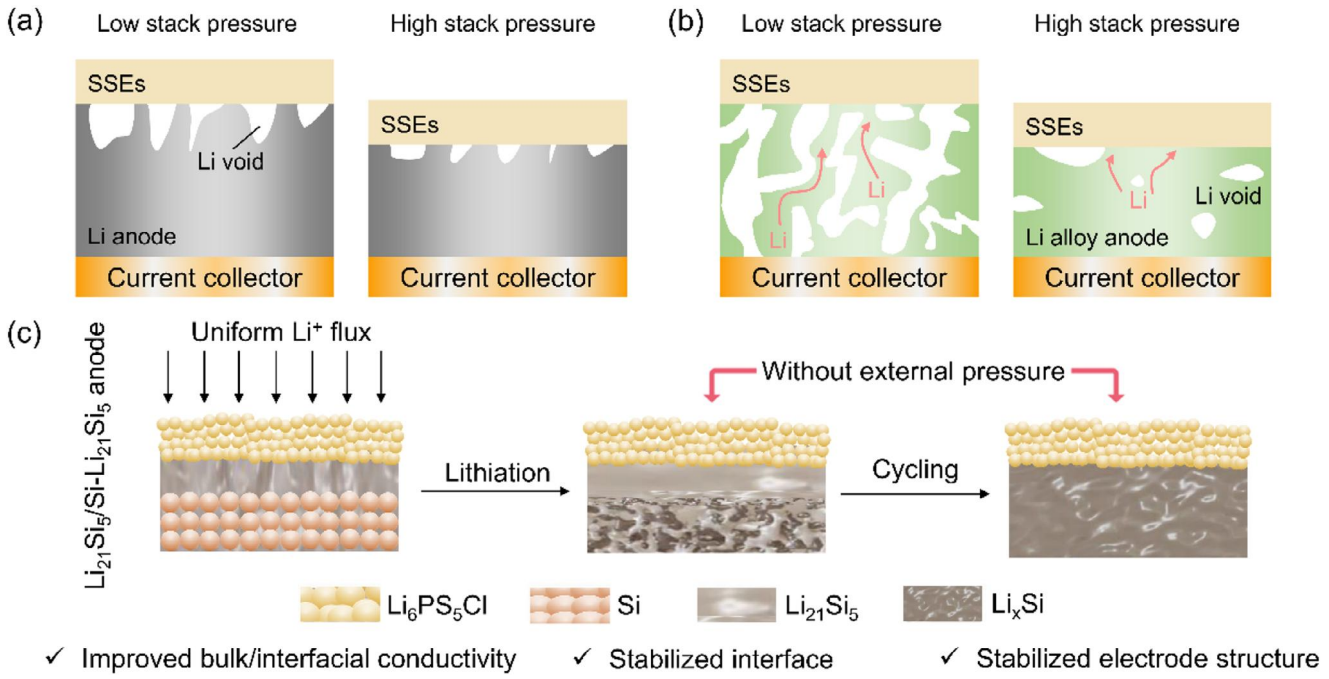

Figure 4. The atomic-scale of anode particles. a) The illustrating stack pressure-dependent Li interface changes during stripping at low stack pressures (<3 MPa) and high stack pressures (3–10 MPa).[65] b) The schematics of dealloying of metallic In at low stack pressures (1 MPa) and high stack pressures (10 MPa).[66] c) The schematics of pressure-free $Li_{21}Si_5$/Si-$Li_{21}Si_5$-ASSBs with stable cycling.[67]

2.3. Solid-State Electrolytes

Solid-state electrolytes (SSEs) in SSLMBs require precise control of stacking pressure to balance ionic conductivity, mechanical stability, and interfacial contacts.[69] Unlike liquid electrolytes, SSEs rely on external pressure to eliminate voids and ensure intimate electrode-electrolyte contact, directly influencing Li^+ transport and dendrite suppression. The effects of external pressure on SSEs are multifaceted; they primarily enhance ionic conductivity through improved particle-to-particle contact within the SSE layer. This mechanism operates without altering the intrinsic ion conduction mechanisms or modifying the fundamental transport properties of the material itself. This improvement stems largely from the reduction of contact resistance through void elimination and particle rearrangement. Simultaneously, the external pressure introduces internal stress within the SSE, which can originate from fabrication-induced particle packing heterogeneity or operational chemo-mechanical mismatches with electrodes. While lattice compression under pressure may slightly increase intrinsic migration barriers, this effect is typically outweighed by the significant gains in contact uniformity and interfacial stability. If unmanaged, however, such internal stress can disrupt ion transport pathways and impair battery performance. Thus, pressure management is critical not only for enhancing interfacial contact but also for mitigating detrimental stress buildup.[56, 58, 70, 71]

As we all know, SSE densification via applied external pressure directly impacts ionic conductivity by reducing porosity and enhancing particle-to-particle contact. For instance, studies on 1-undecanethiol-coated Li_6PS_5Cl (LPSC) SSEs demonstrate that the combination of external pressure and surface lubrication can significantly alter ion transportation: the coating reduces interparticle friction through strong S–S bonding at 375 MPa, thereby enabling particle rearrangement to form a densified structure with 1.7% porosity (vs 10.9% for pristine LPSC). This densification shortens Li^+ pathways, boosting ionic conductivity from 2.61 to 2.93 mS cm^{-2}. Meanwhile, the electronic conductivity remains negligibly low (≈10^{-10} S cm^{-1}), indicating excellent electronic insulation.[72] These results collectively highlight that pressure-induced densification via molecular coatings can suppress dendrite penetration by optimizing both ion transport kinetics and mechanical stability. Building on this experimental foundation, Inoue et al. employed a discrete element model that accounts for plastic deformation to simulate cold pressing of SSEs. Specifically, particle compaction during plastic deformation proceeded through three sequential stages: aggregate breakage, particle rearrangement, and particle consolidation. Notably, higher mold pressure enhanced the relative density while increasing the contact area between active materials and SSEs, with simulation results strongly aligning with experimental observations (**Figure 5a**).[71] Significantly, localized stresses preferentially deformed SSE particles, leading to force concentration at active-material interfaces, a mechanistic insight that theoretically supports the role of particle rearrangement in enhancing ion conduction. Their percolation theory-based conductivity model further highlighted that ball-milled SSE aggregates introduce a critical threshold for continuous ion transport networks, bridging microstructural changes with macroscopic conductivity improvements. Extending the pressure-structure-property relationship, systematic studies on LPSC SSEs reveal distinct morphological and conductive behaviors: low stack pressure leads to sparse contacts and abundant voids between LPSC particles, forming

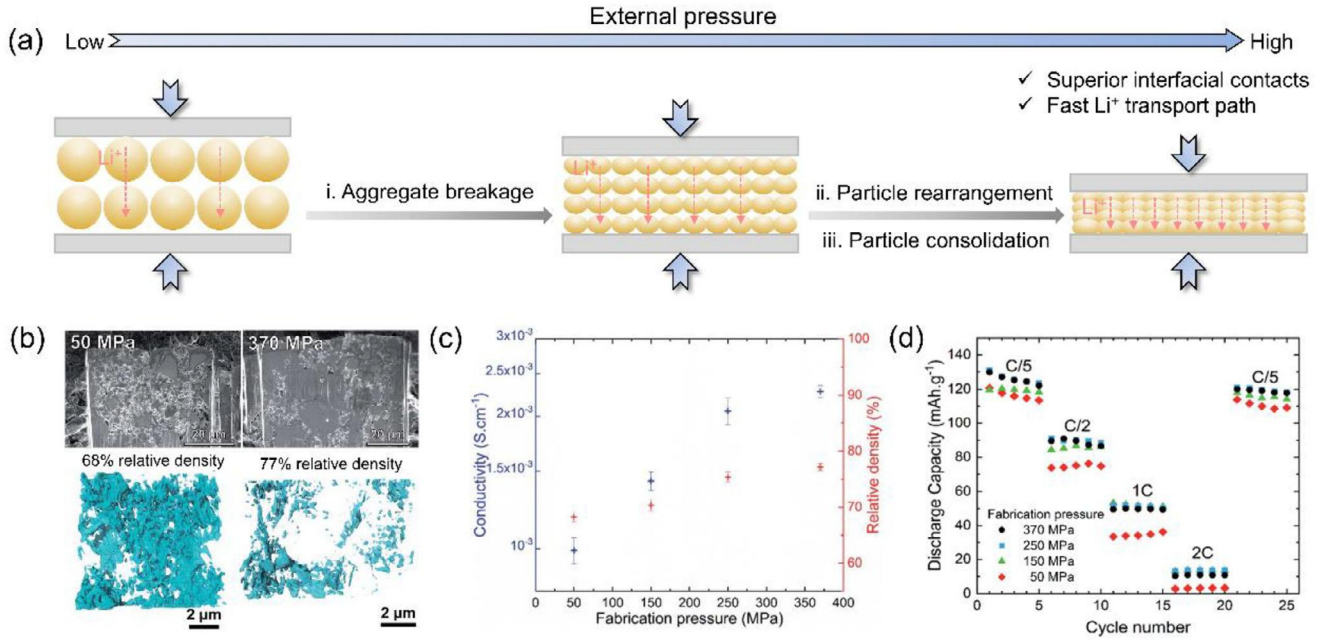

Figure 5. The atomic-scale of solid-state electrolytes. a) The schematics of preparation pressure-induced particle compaction was proceed through three sequential stages: aggregate breakage, particle rearrangement, and consolidation via plastic deformation.[71] b) The cross-sections show pressure-dependent density variations in Li_6PS_5Cl (50/370 MPa) SSE, with porosity mapped in blue. c) The pressure-dependent conductivity and density of Li_6PS_5Cl SSE. d) The pressure-tuned LiIn||LPSC||NCA cells show rate-dependent cycling stability under 25 MPa. Reproduced with permission.[41] Copyright 2020, Royal Society of Chemistry.

discontinuous Li^+ transport pathways. While increasing stack pressure promotes particle rearrangement and consolidation, gradually eliminating voids to establish continuous conductive networks (Figure 5a).[73] This trend corroborates the compaction stage model and provides a practical benchmark for optimizing industrial pressure parameters. Further research differentiates preparation pressure and stack pressure, uncovering dual effects on SSE performance: higher preparation pressure (370 MPa) reduced the porosity of SSEs, with increased relative density correlating to enhance ionic conductivity by minimizing grain boundary impedance (Figure 5b,c). The hard titanium plungers cause poor contact at low preparation pressure, but soft carbon powder as current collectors stabilize electrical conductivity regardless of external pressure. Notably, lower preparation pressure (50 MPa) leads to significantly degraded rate performance at high current density (Figure 5d), whereas higher preparation pressure samples maintain capacity, indicating that optimized preparation pressure enhances ion transport efficiency in SSEs, directly impacting battery rate capability.[41] Beyond cold-pressing approaches, hot-pressing methods leverage combined pressure and temperature to fabricate composite SSEs with unique interfacial structures: the process forms uniform high-modulus vermiculite sheet layers on SSE surfaces (unlike the porous, low-modulus surface of non-hot-pressed electrolytes). The external pressure contributes to a smooth surface for close contact with Li anodes, while suspended vermiculite sheets in the PVDF matrix promote Li salt dissociation and establish efficient Li^+ transport channels.[74] Consequently, demonstrating pressure regulation can extend beyond densification to include interfacial modification, offering versatile strategies for SSE optimization across different processing techniques.

3. Micro-Scale Dynamics: Pressure-Dependent Interfacial Contacts and Li Plating/Stripping Behavior

The atomic-scale pressure effects on ion/electron transport translate to micro-scale dynamics governing electrode/electrolyte interfacial stability and Li plating/stripping behavior. The mechanical pressure dictates the quality of solid–solid interfacial contacts,[75] the evolution of interfacial phases, and the morphological stability of deposited Li during cycling at this scale.[76] In this session, we focus on interfacial contact mechanics and dendrite suppression strategies under external pressure, with particular attention to how external pressure modulates internal stress.[77, 78] This internal stress is the localized force arising from electrochemical reactions, material deformation, or structural mismatches at interfaces and directly influences contact integrity and reaction kinetics.

3.1. Electrode/Electrolyte Interfaces

The interaction dynamics at electrode/SSE interfaces in SSLMBs are profoundly governed by external pressure, which dictates the mechanical coupling, ionic transport, and chemical stability.[79] The pressure-induced densification of composite cathodes modulates the contact area and stress distribution at

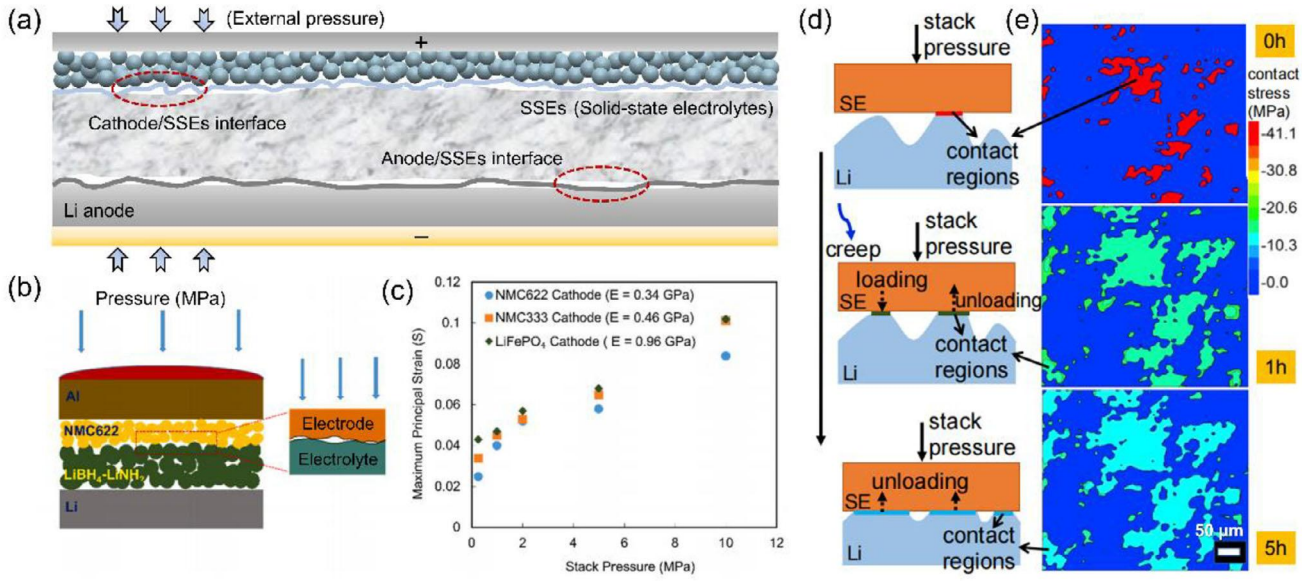

Figure 6. The micro-scale of electrode/electrolyte interfaces. a) The schematic representation of cathode/SEEs interface and anode/SEE interface under external pressure. b) The stack pressure effects on SSLMB interfaces. c) Pressure-induced electrolyte strain distribution. Reproduced with permission.[81] Copyright 2022, Elsevier B. V. d) The behavior of Li creep at Li/solid-state electrolyte (SE) interfaces. e) Li stress distribution at 4.5 MPa (0/1/5 h). Non-contact (blue), stressed regions (red/yellow/green). Reproduced with permission.[82] Copyright 2020, Cell Press.

cathode/SSE interfaces,[80] thereby determining the formation of interphase layers and ion transport pathways in a working battery (**Figure** 6a). Elevated pressures (>100 MPa) enhance mechanical interlocking between cathode particles (NMC, LCO) and sulfide-based SSEs (LPSC), reducing interfacial voids and minimizing charge transfer resistance by counteracting internal stress from cathode volume expansion during cycling. Conversely, excessive pressure can induce microstructural damage in rigid oxide-based cathodes, such as lattice distortion or particle fragmentation, which exacerbates interfacial reactions with oxide-based SSEs (LLZO) and promotes the irreversible decomposition of SSEs. These effects are often driven by amplified internal stress at particle edges where external pressure concentrates.[75–78]

The interplay between pressure and cathode/SSE interfaces is multifaceted, by comparing the effects of single-crystal and polycrystal NMC cathodes under different pressures demonstrates tailored pressure strategies can optimize interfacial contacts and mitigate stress-induced degradation in composite cathodes; high pressure may reduce voids but cause irreversible CEI formation and capacity loss during the initial charge, partly due to internal stress-driven chemical reactions at the interface where mechanical force accelerates side reactions.[57, 83] Based on this, Soboyejo et al. further explored the pressure-strain relationship in $LiBH_4$-$LiNH_2$ systems reveals moderate pressure (0.26 MPa) optimizes interfacial contact with minimal strain, boosting ionic conductivity to 9×10^{-5} S cm^{-1}. In contrast, high pressure (1 MPa) induces excessive axial/shear strains, leading to SSE microcracking and conductivity decline (Figure 6b,c).[81] To mitigate strain-induced contact loss at low pressures, material design strategies have emerged, including surface and bulk modifications that suppress volumetric shrinkage to maintain interfacial continuity, combining low pressure with reduced cutoff voltage to minimize stress-induced voids, and mechanical reinforcement via crosslinked binders that act as scaffolds to sustain contact under cyclic stress, which collectively highlighting the need to synergize densification with chemical stability and strain-resilient materials capable of accommodating internal stress.[58, 84, 85]

For Li anode/SSE interfaces, external pressure exhibits dual effects to moderate stack pressures and promote mechanical wetting as well as uniform Li deposition by minimizing interfacial gaps, thereby relieving internal stress concentration at defect sites where dendrites typically nucleate, while high pressure can induce Li creep through the porosity of SSEs, leading to short-circuit risks (Figure 6a). Recent studies highlight that external pressure also dictates the chemical composition and mechanical properties of the solid-state electrolyte interphase (SEI), with higher pressures favoring the formation of dense, inorganic-rich SEI layers (e.g., LiF/Li_2O) that suppress Li dendrite propagation, whereas low pressure can result in organic-rich, mechanically unstable SEI structures. The interplay between pressure, SSE types (e.g., sulfide vs oxide), and electrode material properties remains a key determinant of interfacial stability, requiring tailored pressure strategies for different systems. For instance, the high stack pressure enhances Li-LLZO adhesion and reduces interfacial resistance by counteracting internal stress from Li volume changes, while low pressure leads to poor contacts with high resistance and weak adhesion. This highlights the role of mechanical compaction in forming robust interfaces where failure occurs within Li metal rather than at the working interface.[86] Subsequently, a "critical stack pressure" balances stripping and creep-driven recovery in Li-LLZO cells, inducing void and resistance growth. Above this threshold, dynamic equilibrium between electrochemical kinetics and mechanical deformation maintains stable contact, underscoring pressure's dual role in balancing ion flux and interfacial mechanics.[87] Building on these findings, a multi-scale model shows that sufficient pressure suppresses

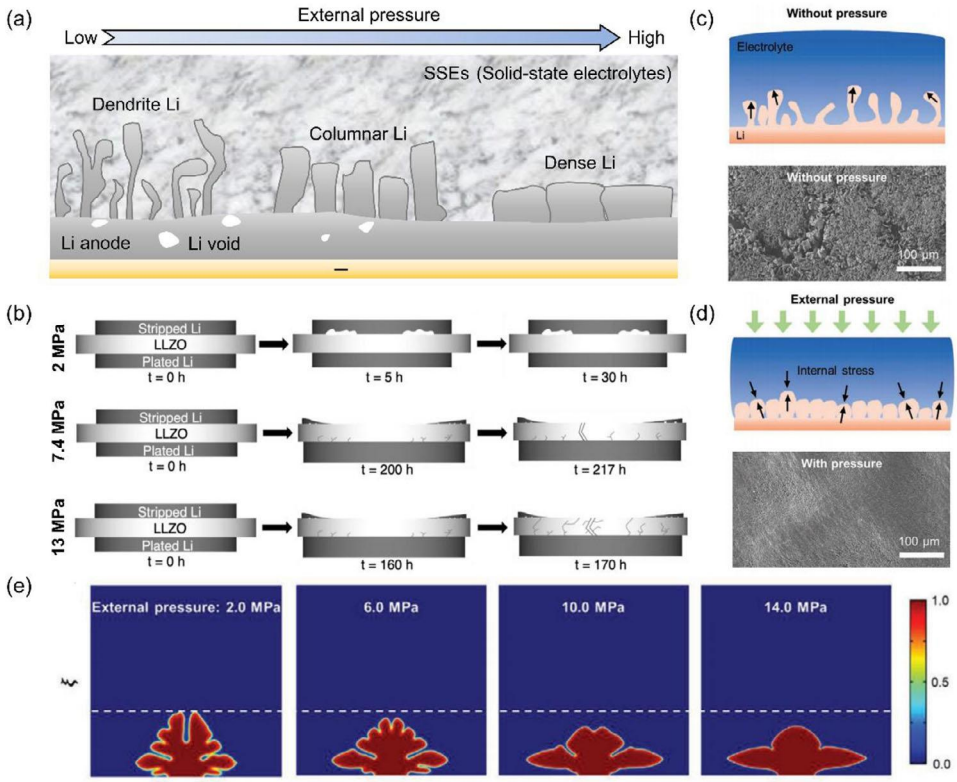

Figure 7. The micro-scale of mechanistic suppression Li dendrites growth. a) The schematic representation of various of deposited Li morphology from low external pressure to high external pressure. b) The schematic of inferred interface evolution of contact loss and void formation under 2/7.4/13 MPa. Reproduced with permission.[52] Copyright 2021, Nature Publication Group. The schematic representation and SEM image of deposited Li c) without pressure and d) with pressure. e) Modeling dendrite evolution under mechanochemical stress (2.0/6.0/10.0/14.0 MPa). Reproduced with permission.[36] Copyright 2021, Wiley-VCH.

voids via conformal contact, homogenizing stress to mitigate Ostwald ripening, while low pressure exacerbates current crowding by allowing internal stress to drive interfacial separation (Figure 6d,e).[82] Furthermore, SSEs exhibit distinct responses to pressure that demand tailored optimization. In LSPS, the moderate stack pressure reduces voids but accelerates interphase formation, whereas the low stack pressure enables Li filaments to grow through pores and cause short circuits.[88] This variability underscores the need to align pressure strategies with SSE type, whether oxide or sulfide, and their inherent stability against Li. Importantly, even high pressure cannot fully eliminate irrecoverable voids from initial stripping cycles in Li-LLZO, revealing fundamental limits to pressure-driven recovery.[37] These limitations highlight the value of material-engineering approaches. Buffer layers form ion-conductive interlayers under moderate pressure to dissipate stress, and carbon interlayers use lamination pressure to tune interfacial toughness, offering effective complements to pressure-based strategies.[89–91]

3.2. Mechanistic Suppression of Dendrites

The inhibition of Li dendrite growth in SSLMBs relies on pressure-induced regulation of mechanical constraints and electrochemical kinetics.[92] The Monroe-Newman criterion suggests SSEs with sufficient shear modulus (exceeding twice that of metallic Li) can theoretically suppress dendrite penetration, but practical limitations arise from the microstructural defects of SSEs (e.g., grain boundaries, pores) that act as preferential growth pathways.[93] External pressure addresses this challenge by homogenizing interfacial stress through elastic deformation of SSEs, thereby reducing localized internal stress concentrations that drive dendrite nucleation. For instance, dynamic pressure coupling during cycling further compensates for volume expansion, minimizing interfacial delamination and crack propagation by relieving cyclic internal stress from Li plating/stripping. The external pressure also modulates Li electrodeposition kinetics[48, 94, 95] by enhancing ion transport efficiency in compacted SSEs, which mitigates the "tip effect" (where concentrated Li^+ flux amplifies internal stress at dendrite tips) and promotes uniform Li plating (**Figure 7a**). An additional fatigue-driven failure mechanism is prosed in Li anodes, where cyclic mechanical loading from repeated Li plating/stripping induces microcrack formation and accelerates dendrite growth by concentrating internal stress at crack tips. This insight underscores the request for pressure regulation that not only suppress initial dendrite nucleation but also mitigate long-term mechanical degradation by balancing external pressure and internal stress evolution. Emerging approaches, such as nanostructured SSE coatings and adaptive pressure systems aim to optimize stress

distribution while mitigating SSE degradation, offering new pathways for dendrite-resistant design of SSLMBs.

Specific experimental studies further confirm the critical role in dendrite suppression. For Li metal anodes with Li_6PS_5Cl SSE, low stack pressure (5 MPa) maintains stable Li plating/stripping by minimizing interfacial voids, while high pressure (75 MPa) triggers short circuits via Li creep through SSE pores. At moderate pressure (25 MPa), dendrites form gradually during cycling due to localized stress from Li creep into electrolyte grains, highlighting the critical role of pressure in balancing mechanical stability and electrochemical kinetics to suppress dendrites.[13] Building on this experimental framework, Harris et al. developed a 3D contact mechanics model to quantify stress homogenization at Li/SSE interfaces, revealing that external pressure homogenizes stress distribution by conforming rough Li surfaces to SSEs, suppressing "tip effect"-induced dendrite nucleation.[35] Complementary in situ observations by Steingart et al. employed *operando* acoustic transmission and ^{7}Li MRI to reveal that low stack pressure (2 MPa) induces rapid interfacial void formation and dendrite growth at Li/LLZO interfaces, while moderate stack pressure (7.4 MPa) suppresses voids via Li creep but promotes lateral Li penetration into electrolyte grain boundaries due to uneven internal stress distribution. At high stack pressure (13 MPa), mechanical failure occurs due to electrolyte cracking, highlighting a critical pressure threshold for balancing contact stability and SSE integrity (Figure 7b).[52] Morphological control mechanisms were further elucidated by Zhang et al. employing a electro-chem- mechanics[96, 97] phase field model to reveal that external pressure reshapes Li dendrites from branched to smooth and dense structures by suppressing tip growth and promoting lateral expansion (Figure 7c,d). However, excessive external pressure (>14 MPa) induces root fractures and dead Li formation due to concentrated von Mises internal stress at dendrite bases (Figure 7e). A pressure-modulus phase diagram is proposed to direct customized strategy formulation, demonstrating low-modulus electrolytes such as 0.5 GPa PP separators necessitate lower critical pressures (6 MPa) to avoid amplifying internal stress, whereas stiffer garnet-type SSEs require elevated pressures to achieve effective dendrite suppression.[36, 98, 99]

While the above experimental and modeling insights underscore the pivotal role of external pressure in dendrite suppression, they also reveal its inherent limitations as a standalone strategy, including gradual dendrite growth under moderate external pressure, mechanical failure at high external pressure, and SSE-type dependent efficacy. In response, researchers are increasingly pursuing integrated approaches that combine pressure with multi-physical field modulation and interfacial engineering to improve suppression efficacy. The influence of pressure on metallic lithium deposition morphology follows a well-defined mechanistic relationship. Below a critical stack pressure (CSP), heterogeneous stress distribution promotes large, irregular dendrites with wide diameter variations due to localized current focusing. Within the optimal pressure range, uniform compressive stress promotes dense, fine-grained lithium deposits with narrower diameter distribution. Exceeding CSP triggers lithium creep, leading to smaller but fragmented deposits that risk short circuits. This dynamic is consistent across electrolyte types, with CSP values varying by SSE mechanical properties (e.g., lower for ductile sulfides vs higher for rigid oxides).[42] Notably, the multi-physical field effects also play a role, as coupled pressure-temperature conditions synergistically suppress dendrites by homogenizing internal stress and enhancing ion transport, though excessive pressure risks stress concentration at dendrite roots, causing fracture and "dead Li" to unbalanced internal stress.[93, 100, 101] Moreover, the interfacial regulation synergizes with pressure regulation by tailoring interfacial properties to amplify pressure's dendrite-suppressing effects while easing its limitations. Such enhancing wettability, blocking electron leakage, stabilizing SEI, or buffering stress, enabling stable cycling under moderate or low external pressure.[94, 102, 103] They create a feedback loop with material engineering boosts pressure's efficacy, while pressure lessens demands on material performance. This synergy expands viable pressure ranges across SSE systems, resolves trade-offs like stress concentration, and strengthens paths to dendrite-resistant SSLMBs.

4. Macro-Scale Engineering and Industrial Application: Dynamic Pressure Coupling Mechanisms and Implementation Advantages

The preceding sections have delved into the foundational role of external pressure in modulating ion/electron transport at the atomic scale and governing interfacial dynamics at the micro-scale in SSLMBs.[104, 105] These mechanistic insights form the basis for translating pressure regulation into macro-scale industrial applications. As we shift focus to characterization of dynamic pressure coupling and industrial implementation strategies, the emphasis transitions from detailed mechanistic analyses to broader technological frameworks that account for how external pressure mitigates or exacerbates internal stress at the pack level. The following sections synthesize these concepts, highlighting how advanced characterization and scalable pressure protocols bridge fundamental science and commercialization.

4.1. Dynamic Pressure Coupling Mechanisms

The integration of in situ and ex situ characterization techniques has been pivotal in decoding the macro-scale interplay between pressure and electrochemical processes in SSLMBs, including their combined effects on internal stress distribution.[106] In situ imaging modalities, including X-ray computed tomography (XCT) and transmission electron microscopy (TEM), have revealed pressure-induced morphological evolutions. These include SSE densification, particle rearrangement, and interfacial behavior evolution, which collectively optimize ion transport pathways while redistributing internal stress from electrode volume changes.[107] Ex situ methods, such as scanning electron microscopy combined with focused ion beam (SEM/FIB) and atomic force microscopy (AFM), have further characterized pressure-dependent microstructural features, such as composite electrode porosity, electrode/SEE dynamic evolution and interfacial stress distributions, providing quantitative insights into how external pressure balances internal stress to maintain contact mechanics (**Figure 8**a). Spectroscopic tools such as X-ray photoelectron spectroscopy (XPS) and nuclear magnetic resonance (NMR) have complemented these by unraveling pressure-induced

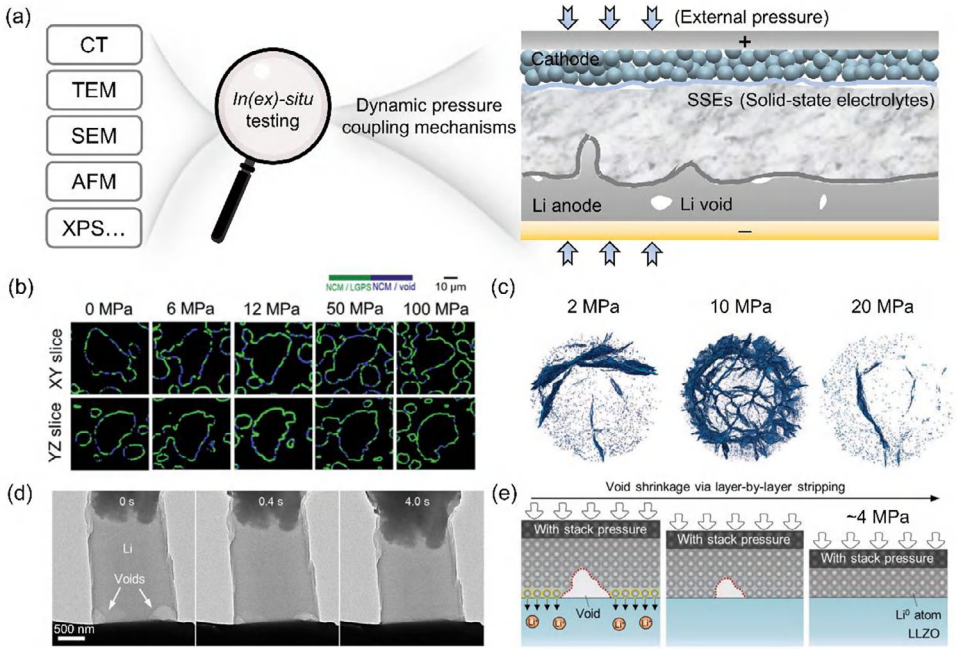

Figure 8. The macro-scale of in (ex) situ dynamic pressure coupling mechanisms. a) The schematic representation of pressure-induced SSLMBs observed via various of characterization techniques. b) Pressure-dependent NCM particle contacts in orthogonal planes at 0/6/12/50/100 MPa. The contacted interfaces of NCM/LGPS (green) and NCM/void (blue). Reproduced with permission.[108] Copyright 2022, Royal Society of Chemistry. c) Pressure-dependent crack propagation in pellets post-short-circuit. Reproduced with permission.[109] Copyright 2025, American Chemical Society. d) The in situ TEM images of stack-pressure-assisted void removal at Li/LLZO interfaces. e) The schematic of void elimination through layer-by-layer stripping. Reproduced with permission.[39] Copyright 2025, American Association for the Advancement of Science.

chemical transformations, including the formation of stable solid-electrolyte interphases (SEIs) that act as internal stress buffers, and enhanced ion dissociation in polymer electrolytes. Together, these techniques have established a multi-scale understanding of how external pressure modulates both the physical structure and chemical reactivity of battery components while managing internal stress, laying the groundwork for rational design of pressure protocol.

Specifically, such characterization approaches have revealed key pressure-related phenomena across studies. In situ XCT and XRD, for instance, visualizes dendritic formations under higher pressures and identifies SEI components, linking morphological and chemical evolutions at the macro-scale.[13] Moreover, ex situ SEM/FIB analysis of electrolytes prepared under varying fabrication pressures shows that lower pressure leads to interconnected voids and smaller grains, while higher pressure results in denser, larger-grain structures.[41] Complementing these findings, integrating in situ pressure monitoring with electrochemical impedance spectroscopy (EIS) and SEM helps distinguish degradation mechanisms such as interphase growth versus filament penetration, providing a macro-scale framework for pressure optimization in SSLMBs.[88] Further focusing on electrode microstructure, Orikasa et al. employed in situ XCT to analyze the 3D structure of composite electrodes in all-solid-state batteries under varying pressures. They revealed that uniaxial pressure induced anisotropic contact between active materials (NCM) and solid-state electrolytes (LGPS), with better contact along the pressure direction (Z-axis) but insufficient horizontal contact. The XCT results showed that higher pressure (up to 100 MPa) reduced porosity in composite electrodes, though tortuosity increased due to particle rearrangement, indicating a trade-off between contact area and ion transport efficiency mediated by internal stress redistribution (Figure 8b).[108] Building on this, *operando* pressure measurement paired with XCT decodes micro-short circuit occurrences in sulfide-based ASSLMBs, identifying two failure modes: minor soft short-circuits (voltage drop with overcharge) and major soft short-circuits (severe voltage fluctuations), correlated with internal stress levels and current densities, and defining a "safety zone" for Li anodes under low stress and current.[110] For a deeper understanding of short-circuit mechanisms, *operando* neutron imaging combined with ex situ XCT further clarifies "soft short-circuit" and "hard short-circuit" mechanisms by tracking real-time Li creep (driven by internal stress gradients), plating-induced stress, and 3D dendrite structures, linking pressure-induced structural changes to failure mechanisms.[111, 112] In addition, Hatzell et al. employed 3D synchrotron imaging and mesoscale modeling to examine solid-state batteries without a lithium reservoir under different levels of stack pressure, which indicated that low stack pressure (2 MPa) leads to irregular Li plating and early failure due to unmitigated internal stress from uneven deposition, while higher stack pressure (20 MPa) induces SSE fractures from tensile stress at surface notches where internal stress exceeds material strength (Figure 8c).[109] Embedded optical fiber sensors monitored interfacial stress dynamics under low stack pressure,[113] and in situ transmission electron microscopy (TEM) visualized void evolution at the Li/LLZO interface with low pressure inducing preferential void nucleation at grain boundaries,

correlated with voltage fluctuations, while higher pressure promotes homogeneous layer-by-layer stripping, suppressing void growth via enhanced mechanical contact and reduced adatom diffusion (Figure 8d,e).[39, 114] Collectively, these characterization efforts bridge pressure-induced structural and chemical changes to battery performance, guiding optimized pressure strategies for stable operation.

4.2. Advantages of External Pressure Implementation in Working Devices

The industrial viability of external pressure application stems from its ability to address three critical challenges in solid-state battery manufacturing: interfacial contact inhomogeneity, dendritic Li growth,[115] and process scalability.[104] Standardized pressure protocols have emerged as a universal strategy to enhance "solid-solid" interface contact quality, leveraging mechanical compaction to reduce voids and create continuous ion-conductive networks in composite electrodes, and mitigate internal stress concentrations that arise from material mismatches during fabrication.[78] Dynamic pressure modulation techniques, such as pulsed or oscillatory pressure, further suppress Li dendrites by disrupting preferential growth kinetics at defect sites, aligning with mechanistic models of stress-driven deposition uniformity. Beyond performance improvements, such pressure-based strategies integrate seamlessly with existing manufacturing infrastructure, including roll-to-roll (R2R) lamination and high-throughput compaction systems, enabling controlled distribution of external force to counteract internal stress across large-area electrodes. These scalable approaches enable the integration of solid electrolytes and electrodes under controlled mechanical conditions, minimizing reliance on high-temperature or solvent-based processes that could exacerbate internal stress through thermal expansion mismatches. From an electric vehicle (EV) industry perspective, pressure regulation supports key performance targets: 1) Enhancing energy density by optimizing interfacial contact to approach 500 Wh kg^{-1}; 2) Extending cycle lifetime through dendrite suppression and stress-induced SEI stabilization; 3) Improving safety by mitigating thermal runaway risks through dynamic pressure modulation that releases excess stress. These benefits are amplified in large-format cells, where uniform pressure distribution addresses scalability challenges unique to EV battery packs.[42] By optimizing pressure parameters, manufacturers can balance electrode material densification with mechanical integrity, reducing internal stress-induced defects such as microcracks and delamination, and paving the way for cost-effective and scalable production of solid-state batteries suitable for EV applications.

The applications of external pressure have been widely employed in SSLMB research to advance industrial adaptability by managing internal stress. Lindström et al. established foundational pressure optimization logic via single-layer pouch cell studies, identifying that moderate external pressure reduces active Li loss and extends cycling lifetime by mitigating internal stress from uneven Li plating (**Figure 9**a,b), providing a critical baseline for standardized protocols.[116] Building on this, researchers focused on material-level pressure adaptability, designing a 3D crosslinked network to achieve superior performance under low stack pressure, shifting pressure dependence from equipment to internal electrode architecture and laying the foundation for low-pressure processes.[85] Furthermore, Brunklaus et al. revealed the pressure sensitivity differences in polymer electrolytes: crosslinked polyethylene oxide (xPEO) balances rate performance and mechanical deformation at ≤0.43 MPa by accommodating internal stress through chain flexibility, while softer xGCD-PCL required pressure-free operation, highlighting the need to match material mechanical strength with pressure requirements for industrial material selection.[117] Device-level innovations have further boosted the scalability of external pressure utilization in solid-state batteries. To ensure meaningful comparison and effective technology transfer from laboratory research to industrial production, a standardized framework for reporting pressure parameters is essential. This framework should include: (1) Clear differentiation between preparation pressure and stack pressure maintained during cycling; (2) Specification of measurement locations (e.g., electrode-electrolyte interfaces) and uniformity metrics across the cell area; (3) Systematic reporting of critical stack pressure (CSP) as a system-specific benchmark, enabling reliable cross-study comparability.[42] To provide practical guidance for researchers and engineers optimizing SSLMB design and operation under external pressure, we have compiled comparative data from multiple studies (**Table 1**). This compilation reveals that polymer-based systems generally function effectively at relatively lower external pressures, while sulfide and oxide-based electrolytes typically require higher pressure ranges. Such systematic pressure characterization and reporting will facilitate the rational selection of pressure parameters tailored to specific material systems and accelerate the development of commercially viable SSLMBs.

For instance, Meng et al. introduced isostatic pouch cell holders (IPCHs) that use air as the pressurizing medium enable uniform pressure control. Testing on $LiNi_{0.8}Co_{0.1}Mn_{0.1}O_2||Li_6PS_5Cl||Si$ pouch cells across 1–5 MPa showed optimal performance at 2 MPa, with 83.6% capacity retention after 100 cycles. Notably, bilayer pouch cell under 5 MPa are not only cycle stable but can even power an incandescent bulb at 3 C, highlighting how IPCHs facilitate industrial scalability through uniform pressure distribution and compatibility with existing infrastructure (Figure 9c,d).[38] Parallel advancements include the design of lithiophilic Mg-SiGr anodes, which direct Li deposition to achieve uniform Li–Mg alloying under 3 MPa, suppressing dendrites without aggressive mechanical loading and opening new avenues for high-energy-density systems.[63] Additionally, continuous application of 0.3 MPa pressure has been shown to recover 57% capacity in aged cells by relieving internal stress-induced voids at interfaces, revealing pressure's untapped potential in battery refurbishment, particularly for second-life applications.[129] Furthermore, the material and process innovations have further expanded the practicality of external pressure application by tuning internal stress responses. A self-limiting multifunctional composite sulfide electrolyte allows sulfide-based all-solid-state lithium-metal pouch cells to operate stably at ≈2 MPa. with 95.04% capacity retention after 500 cycles. Notably, 3D-printed pouch cells with M-CSE achieve an energy density of 219 Wh kg^{-1} under low pressure, demonstrating that rational electrolyte design can optimize stress distribution and mitigate dendrite growth, paving the way

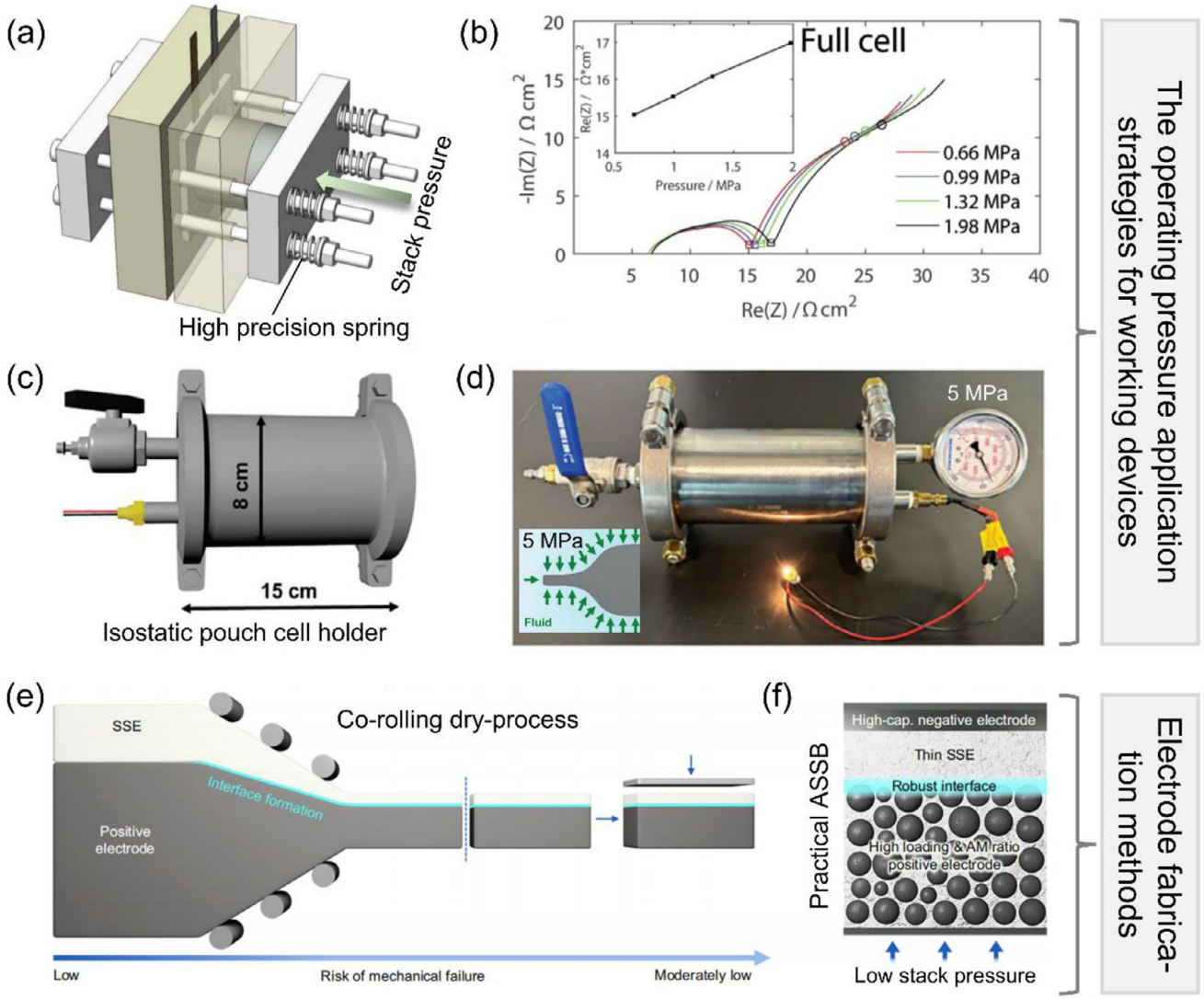

Figure 9. The advantages of external pressure implementation in industrial systems. a–d) The operating pressure application strategies for working devices. a) The precision pressure application via spring-loaded assembly. b) The EIS spectra under varying compressive loads. Reproduced with permission.[116] Copyright 2018, Elsevier B. V. c) The structure of isostatic pouch cell holders (IPCHs). d) The bilayer solid-state cell driving 2.5 V/300 mA load under 5 MPa isostatic pressure. Reproduced with permission.[38] Copyright 2024, Wiley-VCH. e-f) The electrode fabrication methods and their effects. The schematic illustrating of e) co-rolling dry-process and f) practical cell design under low stack pressure. Reproduced with permission.[118] Copyright 2025, Nature Publication Group.

for low-pressure ASSLMB applications.[130] On the industrial application front, Chen et al. developed a co-rolling dry-process that integrates thin SSE layers (50 μm) with high-loading NCM electrodes (5 mAh cm^{-2}) via shear-induced particle interlocking. The co-rolling dry-process enhances volumetric energy density by 20% compared to "non-co-rolled processes" (note: "non-co-rolled" refers to processes without shear-induced particle interlocking during electrode-SSE lamination, not absolute pressure-free. The non-co-rolled cells still underwent a final low-pressure compaction, while the co-rolled cells combined shear lamination with a final pressurization step to achieve denser microstructures (Figure 9e,f). Both types of cells were tested under moderate stack pressure (5–10 MPa) during cycling.[118] The facts above reveal that, the advantages of external pressure are closely tied to its regulatory effects across different scales—from stabilizing microscale electrode-electrolyte interfaces to facilitating macroscale manufacturing. To systematically clarify these multi-scale mechanisms, **Table 2** summarizes the core findings and highlights how preparation and stack pressure modulate structure and electrochemical performance at atomic, micro, and macro levels.

Taken together, these advancements reflect a clear transition in the role of external pressure: from a laboratory-based optimization parameter to an integrated industrial solution. Leading battery manufacturers now recognize pressure management as a critical enabling technology, incorporating dynamic pressure control directly into battery pack designs to balance electrochemical performance with practical constraints. This includes

Table 1. The stack pressure requirements for different types of SSLMBs based on electrolyte materials.

Battery type	Electrolyte material	Full cell and stack pressure	Refs.
Polymer-based	elastic electrolyte	Li||μm-Si & 0 MPa	[107]
	xPEO/xGCD-PCL composite	Li||NMC622 & ≤ 0.43 MPa	[106]
	CPS-6 electrolyte	Li||NCM811 & 1 MPa	[70]
	PVDF-HFP; PVCA	— & 0.1–0.5 MPa	[108]
	PTF-PE-SPE	Li||LRMO & 1 MPa	[32]
Sulfide-based	Li_6PS_5Cl (LPSC)	Li-In||μm-Si & 10 MPa	[107]
	g-C_3N_4@Li_6PS_5Cl	Li||$LiNi_{0.6}Mn_{0.2}Co_{0.2}O_2$ & 30 MPa	[109]
	Li_6PS_5Cl thin film	Li||$Li_4Ti_5O_{12}$ & 2–5 MPa Li-In||S & 2–5 MPa	[110]
	Li_6PS_5Cl	Li-In||NCA & 25 MPa	[36]
	Li_6PS_5Cl	Li||NCM811 & 5–20 MPa	[69]
	UDSH@LPSC	Li||NCM & 30 MPa	[68]
	$Li_{9.54}Si_{1.74}P_{1.44}S_{11.7}Cl_{0.3}$	Li||LTO & 12.7 MPa	[99]
Oxide-based	LLZO	— & 30–40 MPa	[108]
	xLi_2O-MCl_y (M = Ta or Hf, $0.8 \le x \le 2$, y = 5 or 4)	Li-In||$Ni_{0.83}Co_{0.11}Mn_{0.06}O_2$ (NCM-83) & 80 MPa	[111]
	$Li_{1.75}ZrCl_{4.75}O_{0.5}$	Li-In||$LiCoO_2$ (LCO) & 190 MPa	[112]
	$Li_{1.3}Al_{0.3}Ti_{1.7}(PO_4)_3$ (LATP)	$LiFePO_4$-PILG||LATP-PILG|PILG||Li & 20 MPa	[113]
	$Li_{1.3}Al_{0.3}Ti_{1.7}(PO_4)_3$ (LATP)	Li||LATP-Li_3InCl_6·nDMF||Li & 500 MPa	[114]
Ceramic-based	thiophosphate or argyrodite electrolyte	Li||NMC622 & ≥ 5 MPa	[106]
Halide-based	Li_3InCl_6	10Li–Ag_x||10Li–Ag_x & 27 MPa	[115]
	$Li_{3-x}In_{1-x}Zr_xCl_6$	n-type OEMs||NCM83 & 7 MPa	[116]

the adoption of adaptive pressure apparatuses (e.g., pneumatic actuators, spring-loaded fixtures) and process optimization (e.g., R2R lamination with controlled pressure profiles) to reduce reliance on high static pressure, aligning with the shift toward low-pressure or pressure-free systems advocated in academic research.[42, 118] By prioritizing compatibility with existing production infrastructure while intelligently exploiting pressure-stress coupling mechanisms, industry efforts are enhancing manufacturing scalability and end-product reliability, thereby bridging the gap between fundamental research and commercial application.

5. Conclusion and Perspectives

External pressure has evolved from a simple processing parameter to a sophisticated design tool for solid-state lithium-metal batteries (SSLMBs), offering multi-scale control over ion transport, interfacial stability, and mechanical integrity. At the atomic scale, applied pressure densifies solid-state electrolytes (SSEs) microstructures and enhances electrode particle contact while mitigating lattice mismatch-induced internal stresses, which is critical for achieving high active material utilization in composite cathodes. Microscopically, pressure-mediated interfacial engineering promotes the formation of stress-dissipative inorganic-rich interphases that simultaneously suppress Li dendrite propagation and accommodate electrode volume changes. Crucially, macro-scale implementation through roll-to-roll manufacturing and dynamic pressure coupling demonstrates the industrial viability of these principles, enabling interfacial integrity during cycling by actively counterbalancing internal stress evolution. These multi-scale effects collectively demonstrate that external pressure is not merely a mechanical intervention but a versatile tool to harmonize electrochemical kinetics and mechanical stability by managing internal stress, unlocking the potential of SSLMBs for high-energy-density and safe energy storage.

The future roadmap for intelligent pressure engineering is explained in the following aspects:

Table 2. The multi-scale effects of external pressure on SSLMBs.

Scale	Pressure type	Key effects on structure	Key effects on electrochemical performance
Atomic-scale	Preparation pressure	Densifies SSE lattices; reduces particle porosity	Enhances ionic conductivity
	Stack pressure	Optimizes interfacial atom arrangement	Lowers charge transfer resistance
Micro-scale	Preparation pressure	Ensures electrode/SSE interfacial contact	Reduces initial polarization
	Stack pressure	Suppresses Li dendrite growth; stabilizes SEI	Extends cycling lifetime
Macro-scale	Preparation pressure	Enables large-area electrode/SSE fabrication	Improves batch consistency
	Stack pressure	Maintains pack-level interfacial integrity	Enhances volumetric energy density

1) Mechanistic Decoding: The emerging *operando* high-resolution spectroscopy (NMR/XPS) coupled with nanoscale stress mapping will unravel the dynamic relationship between pressure-modulated interfacial chemistry and internal stress redistribution during cycling.
2) Adaptive Control Systems: Closed-loop pressure regulation systems integrating machine learning algorithms with real-time impedance monitoring will enable dynamic pressure adjustments (±5% precision) to counteract stress fluctuations induced by fast charging or thermal transients.
3) Multiscale Modeling: Synergistic 4D visualization combining synchrotron X-ray tomography (50 nm resolution) with phase-field simulations will decode stress-driven failure mechanisms by tracking dendrite nucleation and SSE fracture propagation across cycling conditions.
4) Material-Centric Solutions: Next-generation materials will leverage gradient SSE architectures with spatially tuned mechanical properties (1–10 GPa modulus gradients), dynamic covalent polymer networks enabling 90% self-healing efficiency in composite electrodes, and 3D lithiophilic scaffolds engineered with submicron pore geometries to redistribute interfacial stresses.
5) Sustainable Manufacturing: Dry electrode processing technologies will achieve <100 MPa compaction pressures while maintaining electrode integrity, seamlessly integrating with existing roll-to-roll production lines for gigawatt-scale deployment.
6) Interdisciplinary Integration: Future efforts should focus on merging pressure engineering with smart sensing and AI-driven predictive control, enabling real-time stress compensation and self-adaptive interfacial stabilization without relying on constant external pressure.
7) Material-Process Co-Design: Developing next-generation solid electrolytes and electrode architectures that intrinsically minimize internal stress and pressure dependency through tailored mechanical properties and self-regulating interfaces will be essential for truly pressure-free SSLMBs.
8) Sustainable and Scalable Strategies: Emphasis should be placed on eco-friendly manufacturing processes that integrate pressure optimization with recyclable cell designs, supporting circular economy principles while maintaining high performance under minimal external pressure.

The coming decade will witness a paradigm shift from static "high-pressure fixes" to intelligent pressure management systems that autonomously regulate interfacial stresses. By harmonizing these advances with materials innovation, SSLMBs can achieve the trifecta of energy density (>500 Wh kg^{-1}), cycle life (>1000 cycles), and safety required for electric aviation and grid storage, which ultimately accelerates the post-lithium-ion era.

Acknowledgements

This work was supported by National Key Research and Development Program (No. 2021YFB2500300), Anhui Science and Technology Innovation Tackling Key Problems Plan Project (No. 202423h08050005), National Natural Science Foundation of China (Nos. 22308190, 22393900, 22393904, 52394170, 22409114, 22409113, 22409114), the Beijing Municipal Natural Science Foundation (Nos. L247015, L233004 amd L243019), China Postdoctoral Science Foundation (Nos. 2023M731864 and 2023M731920), and Tsinghua University Initiative Scientific Research Program. P.X. and W.J.K. appreciate the Shuimu Tsinghua Scholar Program of Tsinghua University.

Conflict of Interest

The authors declare no conflict of interest.

Keywords

external pressure, industrial application, interfacial contact, lithium plating/stripping, solid-state lithium metal batteries

Received: August 18, 2025
Revised: September 15, 2025
Published online:

[1] S. Xin, X. Zhang, L. Wang, H. Yu, X. Chang, Y.-M. Zhao, Q. Meng, P. Xu, C.-Z. Zhao, J. Chen, H. Lu, X. Kong, J. Wang, K. Chen, G. Huang, X. Zhang, Y. Su, Y. Xiao, S.-L. Chou, S. Zhang, Z. Guo, A. Du, G. Cui, G. Yang, Q. Zhao, L. Dong, D. Zhou, F. Kang, H. Hong, C. Zhi, et al., *Sci. China Chem.* **2023**, *67*, 13.
[2] J. Adjah, B. Agyei-Tuffour, R. A. Ahmed, D. E. P. Klenam, D. Dodoo-Arhin, E. Nyankson, K. Mensah-Darkwa, W. W. Soboyejo, *Energy Storage Mater.* **2025**, *81*, 104461.
[3] J. Janek, W. G. Zeier, *Nat. Energy* **2016**, *1*, 16141.
[4] J. Mohammadi Moradian, A. Ali, X. Yan, G. Pei, S. Zhang, A. Naveed, K. Shehzad, Z. Shahnavaz, F. Ahmad, B. Yousaf, *Nano-Micro Lett.* **2025**, *17*, 279.
[5] W. Wang, Y. C. Lu, *SusMat* **2023**, *3*, 146.
[6] X.-Y. Hu, P. Xu, S. Deng, J. Lei, X. Lin, Q.-H. Wu, M. Zheng, Q. Dong, *J. Mater. Chem. A* **2020**, *8*, 17056.
[7] P. Xu, X. Lin, Z. Sun, K. Li, W. Dou, Q. Hou, Z. Zhou, J. Yan, M. Zheng, R. Yuan, Q. Dong, *J. Energy Chem.* **2022**, *72*, 186.
[8] X. Liu, P. Xu, J. Zhang, X. Hu, Q. Hou, X. Lin, M. Zheng, Q. Dong, *Small* **2021**, *17*, 2102016.
[9] Z. Li, L. Yu, C. X. Bi, X. Y. Li, J. Ma, X. Chen, X. Q. Zhang, A. Chen, H. Chen, Z. Zhang, L. Z. Fan, B. Q. Li, C. Tang, Q. Zhang, *SusMat* **2024**, *4*, 191.
[10] Y.-X. Li, L.-P. Cui, S. Zhang, P.-F. Sun, C.-D. Fang, Y.-H. Zhang, L.-B. Feng, J.-J. Chen, *EES Batteries* **2025**, *1*, 495.
[11] J. Choi, C. Bak, J. Y. Kim, D. O. Shin, S. H. Kang, Y. M. Lee, Y.-G. Lee, *J. Energy Chem.* **2025**, *105*, 514.
[12] J. Adjah, K. I. Orisekeh, M. Vandadi, R. A. Ahmed, J. Asare, B. Agyei-Tuffour, D. Dodoo-Arhin, E. Nyankson, N. Rahbar, W. O. Soboyejo, *J. Power Sources* **2024**, *613*, 234873.
[13] J. M. Doux, H. Nguyen, D. H. S. Tan, A. Banerjee, X. Wang, E. A. Wu, C. Jo, H. Yang, Y. S. Meng, *Adv. Energy Mater.* **2019**, *10*, 1903253.
[14] B. D. Dandena, D.-S. Tsai, S.-H. Wu, W.-N. Su, B. J. Hwang, *EES Batteries* **2025**, *1*, 692.
[15] W.-J. Kong, C.-Z. Zhao, L. Shen, J.-L. Li, Y.-C. Le, X.-Y. Huang, P. Xu, J.-K. Hu, J.-Q. Huang, Q. Zhang, *EES Batteries* **2025**.
[16] W. Z. Huang, P. Xu, X. Y. Huang, C. Z. Zhao, X. Bie, H. Zhang, A. Chen, E. Kuzmina, E. Karaseva, V. Kolosnitsyn, X. Zhai, T. Jiang, L. Z. Fan, D. Wang, Q. Zhang, *MetalMat* **2023**, *1*, 6.
[17] P. Xu, X. Hu, X. Liu, X. Lin, X. Fan, X. Cui, C. Sun, Q. Wu, X. Lian, R. Yuan, M. Zheng, Q. Dong, *Energy Storage Mater.* **2021**, *38*, 190.
[18] P. Xu, Y. C. Gao, Y. X. Huang, Z. Y. Shuang, W. J. Kong, X. Y. Huang, W. Z. Huang, N. Yao, X. Chen, H. Yuan, C. Z. Zhao, J. Q. Huang, Q. Zhang, *Adv. Mater.* **2024**, *36*, 2409489.

[19] D. H. S. Tan, Y.-T. Chen, H. Yang, W. Bao, B. Sreenarayanan, J.-M. Doux, W. Li, B. Lu, S.-Y. Ham, B. Sayahpour, J. Scharf, E. A. Wu, G. Deysher, H. E. Han, H. J. Hah, H. Jeong, J. B. Lee, Z. Chen, Y. S. Meng, *Science* **2021**, *373*, 1494.
[20] X. Gao, Y. Chen, Z. Zhen, L. Cui, L. Huang, X. Chen, J. Chen, X. Chen, D.-J. Lee, G. Wang, *Nano-Micro Lett.* **2025**, *17*, 140.
[21] P. Shi, Z.-Y. Liu, X.-Q. Zhang, X. Chen, N. Yao, J. Xie, C.-B. Jin, Y.-X. Zhan, G. Ye, J.-Q. Huang, S. Ifan E L, T. Maria-Magdalena, Q. Zhang, *J. Energy Chem.* **2022**, *64*, 172.
[22] K. B. Hatzell, X. C. Chen, C. L. Cobb, N. P. Dasgupta, M. B. Dixit, L. E. Marbella, M. T. McDowell, P. P. Mukherjee, A. Verma, V. Viswanathan, A. S. Westover, W. G. Zeier, *ACS Energy Lett.* **2020**, *5*, 922.
[23] W.-J. Kong, C.-Z. Zhao, L. Shen, S. Sun, X.-Y. Huang, P. Xu, Y. Lu, W.-Z. Huang, J.-L. Li, J.-Q. Huang, Q. Zhang, *J. Am. Chem. Soc.* **2024**, *146*, 28190.
[24] T. Wang, Y. Zhang, X. Huang, P. Su, M. Xiao, S. Wang, S. Huang, D. Han, Y. Meng, *SusMat* **2024**, *4*, 219.
[25] W.-M. Qin, Z. Li, W.-X. Su, J.-M. Hu, H. Zou, Z. Wu, Z. Ruan, Y.-P. Cai, K. Li, Q. Zheng, *Nano-Micro Lett.* **2024**, *17*, 38.
[26] H. Yuan, W. Lin, C. Tian, M. Buga, T. Huang, A. Yu, *Nano-Micro Lett.* **2025**, *17*, 288.
[27] P. Xu, Z.-Y. Shuang, C.-Z. Zhao, X. Li, L.-Z. Fan, A. Chen, H. Chen, E. Kuzmina, E. Karaseva, V. Kolosnitsyn, X. Zeng, P. Dong, Y. Zhang, M. Wang, Q. Zhang, *Sci. China Chem.* **2023**, *67*, 67.
[28] X. Q. Xu, X. B. Cheng, F. N. Jiang, S. J. Yang, D. Ren, P. Shi, H. Hsu, H. Yuan, J. Q. Huang, M. Ouyang, Q. Zhang, *SusMat* **2022**, *2*, 435.
[29] Z. Wu, S. He, C. Zheng, J. Gan, L. She, M. Zhang, Y. Gao, Y. Yang, H. Pan, *eScience* **2024**, *4*, 100247.
[30] F. Zhang, Y. Guo, L. Zhang, P. Jia, X. Liu, P. Qiu, H. Zhang, J. Huang, *eTransportation* **2023**, *15*, 100220.
[31] X. Y. Huang, C. Z. Zhao, W. J. Kong, et al., *Nature* **2025**, https://doi.org/10.1038/s41586-025-09565-z
[32] B. Liu, S. D. Pu, C. Doerrer, D. Spencer Jolly, R. A. House, D. L. R. Melvin, P. Adamson, P. S. Grant, X. Gao, P. G. Bruce, *SusMat* **2023**, *3*, 721.
[33] R. Li, W. Li, A. Singh, D. Ren, Z. Hou, M. Ouyang, *Energy Storage Mater.* **2022**, *52*, 395.
[34] A. Sakuda, A. Hayashi, M. Tatsumisago, *Sci. Rep.* **2013**, *3*, 2261.
[35] X. Zhang, Q. J. Wang, K. L. Harrison, K. Jungjohann, B. L. Boyce, S. A. Roberts, P. M. Attia, S. J. Harris, *J. Electrochem. Soc.* **2019**, *166*, A3639.
[36] X. Shen, R. Zhang, P. Shi, X. Chen, Q. Zhang, *Adv. Energy Mater.* **2021**, *11*, 2003416.
[37] W. Zaman, L. Zhao, T. Martin, X. Zhang, Z. Wang, Q. J. Wang, S. Harris, K. B. Hatzell, *ACS Appl. Mater. Interfaces* **2023**, *15*, 37401.
[38] Y. T. Chen, J. Jang, J. A. S. Oh, S. Y. Ham, H. Yang, D. J. Lee, M. Vicencio, J. B. Lee, D. H. S. Tan, M. Chouchane, A. Cronk, M. S. Song, Y. Yin, J. Qian, Z. Chen, Y. S. Meng, *Adv. Energy Mater.* **2024**, *14*, 2304327.
[39] H. Gao, C. Lin, Y. Liu, J. Shi, B. Zhang, Z. Sun, Z. Li, Y. Wang, M. Yang, Y. Cheng, M.-S. Wang, *Sci. Adv.* **2025**, *11*, adt4666
[40] M. Yamamoto, M. Takahashi, Y. Terauchi, Y. Kobayashi, S. Ikeda, A. Sakuda, *J. Ceram. Soc. Jpn.* **2017**, *125*, 391.
[41] J.-M. Doux, Y. Yang, D. H. S. Tan, H. Nguyen, E. A. Wu, X. Wang, A. Banerjee, Y. S. Meng, *J. Mater. Chem. A* **2020**, *8*, 5049.
[42] Q. Li, H. Liu, Y. Ye, K. J. Li, F. Wu, L. Li, R. Chen, *Nat. Energy* **2025**, *10*, 1064.
[43] Y. Chen, Z. Wang, X. Li, X. Yao, C. Wang, Y. Li, W. Xue, D. Yu, S. Y. Kim, F. Yang, A. Kushima, G. Zhang, H. Huang, N. Wu, Y.-W. Mai, J. B. Goodenough, J. Li, *Nature* **2020**, *578*, 251.
[44] X. Liu, B. Zheng, J. Zhao, W. Zhao, Z. Liang, Y. Su, C. Xie, K. Zhou, Y. Xiang, J. Zhu, H. Wang, G. Zhong, Z. Gong, J. Huang, Y. Yang, *Adv. Energy Mater.* **2021**, *11*, 2003583.
[45] J. Cui, X. Chen, Z. Zhou, M. Zuo, Y. Xiao, N. Zhao, C. Shi, X. Guo, *Mater. Today Energy* **2021**, *20*, 100632.
[46] X. Hu, Z. Zhang, X. Zhang, Y. Wang, X. Yang, X. Wang, M. Fayena-Greenstein, H. A. Yehezkel, S. Langford, D. Zhou, B. Li, G. Wang, D. Aurbach, *Nat. Rev. Mater.* **2024**, *9*, 305.
[47] G. Harper, R. Sommerville, E. Kendrick, L. Driscoll, P. Slater, R. Stolkin, A. Walton, P. Christensen, O. Heidrich, S. Lambert, A. Abbott, K. Ryder, L. Gaines, P. Anderson, *Nature* **2019**, *575*, 75.
[48] H. Xu, S. Yang, B. Li, *Adv. Energy Mater.* **2024**, *14*, 2303539.
[49] X. Li, J. Liang, J. Luo, M. Norouzi Banis, C. Wang, W. Li, S. Deng, C. Yu, F. Zhao, Y. Hu, T.-K. Sham, L. Zhang, S. Zhao, S. Lu, H. Huang, R. Li, K. R. Adair, X. Sun, *Energy Environ. Sci.* **2019**, *12*, 2665.
[50] L. Zhang, T. Yang, C. Du, Q. Liu, Y. Tang, J. Zhao, B. Wang, T. Chen, Y. Sun, P. Jia, H. Li, L. Geng, J. Chen, H. Ye, Z. Wang, Y. Li, H. Sun, X. Li, Q. Dai, Y. Tang, Q. Peng, T. Shen, S. Zhang, T. Zhu, J. Huang, *Nat. Nanotech.* **2020**, *15*, 94.
[51] A. M. Bates, Y. Preger, L. Torres-Castro, K. L. Harrison, S. J. Harris, J. Hewson, *Joule* **2022**, *6*, 742.
[52] W. Chang, R. May, M. Wang, G. Thorsteinsson, J. Sakamoto, L. Marbella, D. Steingart, *Nat. Commun.* **2021**, *12*, 6369.
[53] W. J. Kong, C. Z. Zhao, S. Sun, L. Shen, X. Y. Huang, P. Xu, Y. Lu, W. Z. Huang, J. Q. Huang, Q. Zhang, *Adv. Mater.* **2023**, *36*, 2310738.
[54] L. Shen, J. L. Li, W. J. Kong, C. X. Bi, P. Xu, X. Y. Huang, W. Z. Huang, F. Fu, Y. C. Le, C. Z. Zhao, H. Yuan, J. Q. Huang, Q. Zhang, *Adv. Funct. Mater.* **2024**, *34*, 2408571.
[55] Z. Y. Wang, C. Z. Zhao, N. Yao, Y. Lu, Z. Q. Xue, X. Y. Huang, P. Xu, W. Z. Huang, Z. X. Wang, J. Q. Huang, Q. Zhang, *Angew. Chem., Int. Ed.* **2024**, *64*, 202414524.
[56] K. G. Naik, M. K. Jangid, B. S. Vishnugopi, N. P. Dasgupta, P. P. Mukherjee, *Adv. Energy Mater.* **2024**, *15*, 2403360.
[57] C. Doerrer, I. Capone, S. Narayanan, J. Liu, C. R. M. Grovenor, M. Pasta, P. S. Grant, *ACS Appl. Mater. Interfaces* **2021**, *13*, 37809.
[58] X. Gao, B. Liu, B. Hu, Z. Ning, D. S. Jolly, S. Zhang, J. Perera, J. Bu, J. Liu, C. Doerrer, E. Darnbrough, D. Armstrong, P. S. Grant, P. G. Bruce, *Joule* **2022**, *6*, 636.
[59] W.-Z. Huang, Z.-Y. Liu, P. Xu, W.-J. Kong, X.-Y. Huang, P. Shi, P. Wu, C.-Z. Zhao, H. Yuan, J.-Q. Huang, Q. Zhang, *J. Mater. Chem. A* **2023**, *11*, 12713.
[60] C. Xu, Z. Ahmad, A. Aryanfar, V. Viswanathan, J. R. Greer, *Proc. Natl. Acad. Sci. U.S.A.* **2016**, *114*, 57.
[61] A. Masias, N. Felten, R. Garcia-Mendez, J. Wolfenstine, J. Sakamoto, *J. Mater. Sci.* **2018**, *54*, 2585.
[62] S. Y. Han, C. Lee, J. A. Lewis, D. Yeh, Y. Liu, H.-W. Lee, M. T. McDowell, *Joule* **2021**, *5*, 2450.
[63] J. Oh, D. Kwon, S. H. Choi, N. Lee, Y. Sohn, T. Lee, T. Lee, J. Y. Kim, K. Y. Bae, J. W. Choi, *Adv. Energy Mater.* **2024**, *15*, 2404817.
[64] D.-B. Seo, D. Kim, M.-R. Kim, J. Kwon, H. J. Kook, S. Kang, S. Yim, S. S. Lee, D. O. Shin, K.-S. An, S. Park, *Nano-Micro Lett.* **2025**, *17*, 224.
[65] C. G. Haslam, J. K. Eckhardt, A. Ayyaswamy, B. S. Vishnugopi, T. Fuchs, D. W. Liao, N. P. Dasgupta, P. P. Mukherjee, J. Janek, J. Sakamoto, *Adv. Energy Mater.* **2024**, *15*, 2403614.
[66] C. Wang, Y. Liu, W. J. Jeong, T. Chen, M. Lu, D. L. Nelson, E. P. Alsaç, S. G. Yoon, K. A. Cavallaro, S. Das, D. Majumdar, R. Gopalaswamy, S. Xia, M. T. McDowell, *Nat. Mater.* **2025**, *24*, 907.
[67] Z. Zhang, X. Zhang, Y. Liu, C. Lan, X. Han, S. Pei, L. Luo, P. Su, Z. Zhang, J. Liu, Z. Gong, C. Li, G. Lin, C. Li, W. Huang, M.-S. Wang, S. Chen, *Nat. Commun.* **2025**, *16*, 1013.
[68] S. Jun, G. Lee, Y. B. Song, H. Lim, K. H. Baeck, E. S. Lee, J. Y. Kim, D. W. Kim, J. H. Park, Y. S. Jung, *Small* **2024**, *20*, 2309437.
[69] L. Wang, J. Wu, C. Bao, Z. You, Y. Lu, Z. Wen, *SusMat* **2024**, *4*, 72.
[70] M. J. Counihan, Z. D. Hood, H. Zheng, T. Fuchs, L. Merola, M. Pavan, S. L. Benz, T. Li, A. Baskin, J. Park, J. H. Stenlid, X. Chen,

D. P. Phelan, J. W. Lawson, J. G. Connell, J. Janek, F. H. Richter, S. Tepavcevic, *Adv. Energy Mater.* **2025**, *15*, 2406020.
[71] M. So, G. Inoue, R. Hirate, K. Nunoshita, S. Ishikawa, Y. Tsuge, *J. Power Sources* **2021**, *508*, 230344.
[72] M. Liu, E. Lu, S. Wang, S. Feng, J. Gao, W. Yan, J. W. Oh, M.-S. Song, J. Luo, P. Liu, *ACS Energy Lett.* **2025**, *10*, 1389.
[73] J. Sang, B. Tang, Y. Qiu, Y. Fang, K. Pan, Z. Zhou, *Energy Environ. Mater.* **2023**, *7*, 12670.
[74] Z. Yang, B. Yang, S. Wang, J. Qian, Z. Hou, X. Li, *Angew. Chem., Int. Ed.* **2025**, *64*, 202423227.
[75] J. Liu, Q. Zhang, Y. Feng, W. Xia, J. Yan, Z. Liu, J. Zhou, *J. Power Sources* **2025**, *646*, 237268.
[76] A.-L. Yue, H. Yuan, S.-J. Yang, J.-K. Hu, X.-L. Wang, D.-C. Wu, Z.-H. Zuo, B.-D. Bi, Z.-H. Fu, J.-Q. Huang, *J. Energy Chem.* **2025**, *107*, 277.
[77] H. X. Nan, C.-Z. Zhao, H. Yuan, Y. Lu, X. Shen, G.-L. Zhu, Q.-B. Liu, J.-Q. Huang, Q. Zhang, *CIESC J.* **2021**, *72*, 61.
[78] J. Zhang, J. Fu, P. Lu, G. Hu, S. Xia, S. Zhang, Z. Wang, Z. Zhou, W. Yan, W. Xia, C. Wang, X. Sun, *Adv. Mater.* **2024**, *37*, 2413499.
[79] A. Banerjee, X. Wang, C. Fang, E. A. Wu, Y. S. Meng, *Chem. Rev.* **2020**, *120*, 6878.
[80] X.-Y. Zhang, Y. Bao, *J. Electrochem. Soc.* **2025**, *172*, 050515.
[81] R. A. Ahmed, N. Ebechidi, I. Reisya, K. Orisekeh, A. Huda, A. Bello, O. K. Oyewole, W. O. Soboyejo, *J. Power Sources* **2022**, *521*, 230939.
[82] X. Zhang, Q. J. Wang, K. L. Harrison, S. A. Roberts, S. J. Harris, *Cell Rep. Phys. Sci.* **2020**, *1*, 100012.
[83] R. Koerver, I. Aygün, T. Leichtweiß, C. Dietrich, W. Zhang, J. O. Binder, P. Hartmann, W. G. Zeier, J. Janek, *Chem. Mater.* **2017**, *29*, 5574.
[84] W. Zhao, Y. Zhang, N. Sun, Q. Liu, H. An, Y. Song, B. Deng, J. Wang, G. Yin, F. Kong, S. Lou, J. Wang, *ACS Energy Lett.* **2023**, *8*, 5050.
[85] T. Y. Kwon, K. T. Kim, D. Y. Oh, Y. B. Song, S. Jun, Y. S. Jung, *Energy Storage Mater.* **2022**, *49*, 219.
[86] M. Wang, J. Sakamoto, *J. Power Sources* **2018**, *377*, 7.
[87] M. J. Wang, R. Choudhury, J. Sakamoto, *Joule* **2019**, *3*, 2165.
[88] C. Lee, S. Y. Han, J. A. Lewis, P. P. Shetty, D. Yeh, Y. Liu, E. Klein, H.-W. Lee, M. T. McDowell, *ACS Energy Lett.* **2021**, *6*, 3261.
[89] H. Yan, K. Tantratian, K. Ellwood, E. T. Harrison, M. Nichols, X. Cui, L. Chen, *Adv. Energy Mater.* **2021**, *12*, 2102283.
[90] X. Wang, X. Xu, W. Hou, Y. Chen, Y. Yang, Y. Wang, Z. Guo, Z. Song, Y. Liu, *Adv. Energy Mater.* **2024**, *15*, 2402731.
[91] D. W. Liao, D. Zeng, M. Mulla, A. Madanchi, H. Kawakami, Y. Aihara, K. Aotani, M. D. Thouless, N. P. Dasgupta, *Adv. Mater.* **2025**, *37*, 2502114.
[92] J. Yu, X. Sun, X. Shen, D. Zhang, Z. Xie, N. Guo, Y. Wang, *Energy Storage Mater.* **2025**, *76*, 104134.
[93] X. Hu, J. Yu, Y. Wang, W. Guo, X. Zhang, M. Armand, F. Kang, G. Wang, D. Zhou, B. Li, *Adv. Mater.* **2023**, *36*, 2308275.
[94] R. Xiong, H. Li, B.-A. Mei, H. He, W. Shen, *J. Energy Chem.* **2025**, *102*, 734.
[95] Y. Yang, X.-L. Zhong, L. Xu, Z.-L. Yang, C. Yan, J.-Q. Huang, *J. Energy Chem.* **2024**, *97*, 453.
[96] S. E. Sandoval, C. G. Haslam, B. S. Vishnugopi, D. W. Liao, J. S. Yoon, S. H. Park, Y. Wang, D. Mitlin, K. B. Hatzell, D. J. Siegel, P. P. Mukherjee, N. P. Dasgupta, J. Sakamoto, M. T. McDowell, *Nat. Mater.* **2025**, *24*, 673.
[97] C. Yuan, J. Wu, W. Zhang, M. Han, Y. Jia, *J. Energy Chem.* **2025**, *108*, 495.
[98] P. Hou, J. Xie, J. Li, P. Zhang, Z. Li, W. Hao, J. Tian, Z. Wang, F. Li, *Acta Phys. Sin.* **2025**, *74*, 070201.
[99] X. Shen, R. Zhang, P. Shi, X.-Q. Zhang, X. Chen, C.-Z. Zhao, P. Wu, Y.-M. Guo, J.-Q. Huang, Q. Zhang, *Fundamental Research* **2024**, *4*, 1498.
[100] H. Yang, Z. Wang, *J. Solid State Electrochem.* **2023**, *27*, 2607.
[101] L. T. Gao, Y. Lyu, Z.-S. Guo, *ACS Appl. Mater. Interfaces* **2023**, *15*, 58416.
[102] W. Zhang, Z. Wang, H. Wan, A.-M. Li, Y. Liu, S.-C. Liou, K. Zhang, Y. Ren, C. Jayawardana, B. L. Lucht, C. Wang, *Nat. Mater.* **2025**, *24*, 414.
[103] H. Wan, Z. Wang, W. Zhang, X. He, C. Wang, *Nature* **2023**, *623*, 739.
[104] M. Šedina, A. Šimek, J. Báňa, T. Kazda, *Monatsh. Chem.* **2024**, *155*, 221.
[105] Y. Zhu, Y. Wang, M. Xu, Y. Wu, W. Tang, D. Zhu, Y.-S. He, Z.-F. Ma, L. Li, *Acta Physico Chimica Sinica* **2021**, *39*, 2110040.
[106] Y. Zhong, X. Zhang, Y. Zhang, P. Jia, Y. Xi, L. Kang, Z. Yu, *SusMat* **2024**, *4*, 190.
[107] T. Yi, E. Zhao, Y. He, T. Liang, H. Wang, *eScience* **2024**, *4*, 100182.
[108] Y. Sakka, H. Yamashige, A. Watanabe, A. Takeuchi, M. Uesugi, K. Uesugi, Y. Orikasa, *J. Mater. Chem. A* **2022**, *10*, 16602.
[109] S. H. Park, A. Ayyaswamy, J. Gjerde, W. B. Andrews, B. S. Vishnugopi, M. Drakopoulos, N. T. Vo, Z. Zhong, K. Thornton, P. P. Mukherjee, K. B. Hatzell, *ACS Energy Lett.* **2025**, *10*, 1174.
[110] J. Gu, X. Chen, Z. He, Z. Liang, Y. Lin, J. Shi, Y. Yang, *Adv. Energy Mater.* **2023**, *13*, 2302643.
[111] D. Cao, K. Zhang, W. Li, Y. Zhang, T. Ji, X. Zhao, E. Cakmak, J. Zhu, Y. Cao, H. Zhu, *Adv. Funct. Mater.* **2023**, *33*, 2307998.
[112] Z. Ning, G. Li, D. L. R. Melvin, Y. Chen, J. Bu, D. Spencer-Jolly, J. Liu, B. Hu, X. Gao, J. Perera, C. Gong, S. D. Pu, S. Zhang, B. Liu, G. O. Hartley, A. J. Bodey, R. I. Todd, P. S. Grant, D. E. J. Armstrong, T. J. Marrow, C. W. Monroe, P. G. Bruce, *Nature* **2023**, *618*, 287.
[113] G. Li, T. Zhang, J. Tang, M. Liu, Y. Xie, J. Yu, X. Hui, C. Deng, X. Lu, Y. Kim, J. Huang, Z. L. Xu, *Adv. Mater.* **2025**, *37*, 2417770.
[114] L. Zhao, M. Feng, C. Wu, L. Guo, Z. Chen, S. Risal, Q. Ai, J. Lou, Z. Fan, Y. Qi, Y. Yao, *Nat. Commun.* **2025**, *16*, 4283.
[115] H. Liu, X. Sun, X. B. Cheng, C. Guo, F. Yu, W. Bao, T. Wang, J. Li, Q. Zhang, *Adv. Energy Mater.* **2022**, *12*, 2202518.
[116] A. S. Mussa, M. Klett, G. Lindbergh, R. W. Lindström, *J. Power Sources* **2018**, *385*, 18.
[117] P. Roering, G. M. Overhoff, K. L. Liu, M. Winter, G. Brunklaus, *ACS Appl. Mater. Interfaces* **2024**, *16*, 21932.
[118] D. J. Lee, Y. Jeon, J.-P. Lee, L. Zhang, K. H. Koh, F. Li, A. U. Mu, J. Wu, Y.-T. Chen, S. McNulty, W. Tang, M. Vicencio, D. Xu, J. Kim, Z. Chen, *Nat. Commun.* **2025**, *16*, 4200.
[119] H. Pan, L. Wang, Y. Shi, C. Sheng, S. Yang, P. He, H. Zhou, *Nat. Commun.* **2024**, *15*, 2263.
[120] X. Zhang, C. Luo, N. Menga, H. Zhang, Y. Li, S.-P. Zhu, *Cell Rep. Phys. Sci.* **2023**, *4*, 101328.
[121] M. Luo, C. Wang, Y. Duan, X. Zhao, J. Wang, X. Sun, *Energy Environ. Mater.* **2024**, *7*, 12753.
[122] G. L. Zhu, C. Z. Zhao, H. J. Peng, H. Yuan, J. K. Hu, H. X. Nan, Y. Lu, X. Y. Liu, J. Q. Huang, C. He, J. Zhang, Q. Zhang, *Adv. Funct. Mater.* **2021**, *31*, 2101985.
[123] S. Zhang, F. Zhao, J. Chen, J. Fu, J. Luo, S. H. Alahakoon, L.-Y. Chang, R. Feng, M. Shakouri, J. Liang, Y. Zhao, X. Li, L. He, Y. Huang, T.-K. Sham, X. Sun, *Nat. Commun.* **2023**, *14*, 3780.
[124] L. Hu, J. Wang, K. Wang, Z. Gu, Z. Xi, H. Li, F. Chen, Y. Wang, Z. Li, C. Ma, *Nat. Commun.* **2023**, *14*, 3807.
[125] B. Nie, T.-W. Wang, S. W. Lee, J. Zhang, H. Sun, *Mater. Today Energy* **2025**, *49*, 101829.
[126] B. Nie, T.-W. Wang, S. W. Lee, H. Sun, *ACS Appl. Mater. Interfaces* **2024**, *16*, 67635.
[127] F. Liu, T. Cai, Y. Zhu, T. Bai, M. Nie, W. Gan, D. Li, L. Ci, Q. Yuan, *J. Power Sources* **2025**, *647*, 237357.
[128] Y. Hu, H. Su, J. Fu, J. Luo, Q. Yu, F. Zhao, W. Li, S. Deng, Y. Liu, Y. Yuan, Y. Gan, Y. Wang, J. T. Kim, N. Chen, M. Shakouri, X. Hao, Y. Gao, T. Pang, N. Zhang, M. Jiang, X. Li, Y. Zhao, J. Tu, C. Wang, X. Sun, *Nat. Chem.* **2025**, *17*, 1313.

[129] A. Chahbaz, Y. Luo, G. Stahl, H. Ditler, T. Jaumann, M. Glinka, C. Lingen, D. U. Sauer, W. Li, *Adv. Funct. Mater.* **2024**, *35*, 2419229.

[130] F. Xu, Y. Wu, L. Wang, Z. Zhang, G. Liu, C. Guo, D. Wu, C. Yi, J. Luo, W. He, C. Xu, M. Yang, H. Li, L. Chen, F. Wu, *Adv. Energy Mater.* **2025**, *15*, 2405369.

Pan Xu received his B.S. from Nanchang University at 2017 and Ph.D. from Xiamen University at 2022. He joined Prof. Qiang Zhang's group at Tsinghua University as an assistant researcher in 2022-2025. He then joined the School of Chemistry, Xi';an Jiaotong University in June 2025. His research focuses on polymer solid-state electrolytes and Li/Na metal anodes.

Chen-Zi Zhao received her B.S. in Materials Science and Engineering at 2015 and Ph.D. in Chemical Engineering at 2020 from Tsinghua University. Her work explores lithium-ion transport and interfacial chemistry in solid-state lithium batteries, with the goal of enabling highenergy-density, intrinsically safe energy storage.

Qiang Zhang is a professor at Tsinghua University. His current research interests are advanced energy materials and energy chemistry, including Li metal anodes, LiS batteries, and electrocatalysts. He is the Advisor Editor of Angewandte Chemie. He is sitting on the advisory board of Matter, ChemSocRev, Advanced Energy Materials, ChemSusChem, Journal of Materials Chemistry A, Batteries & Supercaps, and so on.